Human Molecular Genetics, 2004, Vol. 13, No. 18 **2043–2059**
doi:10.1093/hmg/ddh209
Advance Access published on July 14, 2004

Epileptic-like convulsions associated with LIS-1 in the cytoskeletal control of neurotransmitter signaling in *Caenorhabditis elegans*

Shelli N. Williams, Cody J. Locke, Andrea L. Braden, Kim A. Caldwell and Guy A. Caldwell*

Department of Biological Sciences, The University of Alabama, Tuscaloosa, AL 35487-0344, USA

Received May 6, 2004; Revised and Accepted July 1, 2004

Cortical malformations are a collection of disorders affecting brain development. Mutations in the *LIS1* gene lead to a disorganized and smooth cerebral cortex caused by failure in neuronal migration. Among the clinical consequences of lissencephaly are mental retardation and intractable epilepsy. It remains unclear whether the seizures result from aberrant neuronal placement, disruption of intrinsic properties of neurons, or both. The nematode *Caenorhabditis elegans* offers an opportunity to study such convulsions in a simple animal with a defined nervous system. Here we show that convulsions mimicking epilepsy can be induced by a mutation in a *C. elegans lis-1* allele (*pnm-1*), in combination with a chemical antagonist of gamma-aminobutyric acid (GABA) neurotransmitter signaling. Identical convulsions were obtained using *C. elegans* mutants defective in GABA transmission, whereas none of these mutants or the antagonist alone caused convulsions, indicating a threshold was exceeded in response to this combination. Crosses between *pnm-1* and fluorescent marker strains designed to exclusively illuminate either the processes of GABAergic neurons or synaptic vesicles surprisingly showed no deviations in neuronal architecture. Instead, presynaptic defects in GABAergic vesicle distribution were clearly evident and could be phenocopied by RNAi directed against cytoplasmic dynein, a known LIS1 interactor. Furthermore, mutations in UNC-104, a neuronal-specific kinesin, and SNB-1, a synaptic vesicle-associated protein termed synaptobrevin, exhibit similar convulsion phenotypes following chemical induction. Taken together, these studies establish *C. elegans* as a system to investigate subtle cytoskeletal mechanisms regulating intrinsic neuronal activity and suggest that it may be possible to dissociate the epileptic consequences of lissencephaly from the more phenotypically overt cortical defects associated with neuronal migration.

INTRODUCTION

Lissencephaly is a rare childhood birth defect of the brain resulting in a smooth cerebral cortex. Lissencephalic brains present with reduced surface area and a lack of cortical folds; this malformation is presumably caused by defects in migration of neurons from the periventricular zone to the cortical plate during development (1). Classical or Type I lissencephaly consists of a subgroup of human neuronal migration disorders including isolated lissencephaly sequence (ILS) and Miller–Dieker syndrome (MDS). When compared with ILS, MDS is generally considered to be a more severe form of classical lissencephaly and includes craniofacial anomalies and other organ malformations (2). ILS and MDS often result from haploinsufficiency at human chromosome 17p13.3; this chromosomal region includes the *LIS1* gene. This gene is disrupted in both ILS and MDS patients and suggests that mutations within *LIS1* are responsible for defective neuronal migration (3). ILS patients typically have point mutations or intragenic deletions within the *LIS1* locus (4,5) whereas MDS patients have deletions within the region of 17p13.3 that includes both *LIS1* and *Ywhae* (14-3-3ε) (2,6–8). *LIS1* encodes the non-catalytic subunit of platelet-activating factor acetyl hydrolase isoform 1B (PAFAH1B) (9,10); this enzyme inactivates platelet activating factor (PAF) and is brain specific. It is not known whether the enzymatic function

*To whom correspondence should be addressed at: Department of Biological Sciences, The University of Alabama, Box 870344, Tuscaloosa, AL 35487-0344, USA. Tel: +1 2053489926; Fax: +1 2053481786; Email: gcaldwel@bama.ua.edu

of LIS1 is important for neuronal migration; however, PAF activity on neurons has been reported (11–13).

The first indication of a possible cellular function for LIS1 came from its identification in the fungus *Aspergillus nidulans*, where a LIS1 homolog termed NUDF was shown to be essential for regulating nuclear distribution and migration in growing hyphae (14). Additional homologs have since been characterized in multiple eukaryotic model organisms, including mouse, rat, *Drosophila melanogaster* and *Caenorhabditis elegans* (reviewed in 15,16). Studies in these organisms have shown that LIS1 proteins also function in nuclear positioning and cell proliferation. For example, LIS1 functions in *Drosophila* neuroblasts (17), *C. elegans* mitotically dividing embryos (18) and cultured mammalian cells (19,20). These cumulative studies have shown that LIS1 is associated with many subcellular structures, including centrosomes, microtubules, the cell cortex and kinetochores, and that LIS1 is important for accurate chromosome segregation. Diverse functions for LIS1 are not surprising as this protein is a member of the WD-40 repeat family of proteins that are characteristically involved in multiple protein–protein interactions.

Through a combination of genetics, *in vitro* and *in vivo* studies, LIS1 has been shown to interact with several proteins associated with the cytoskeleton (reviewed in 15,16). LIS1 colocalizes and interacts with NUDEL and mNudE at the centrosome and regulates cytoplasmic dynein motor function (21–25). Cytoplasmic dynein has been implicated in many cellular mechanisms, including the regulation of intracellular transport of organelles and cytoskeletal components, and retrograde axonal transport. LIS1 interaction with cytoplasmic dynein is important for at least a subset of dynein functions, including mitotic progression and retrograde movement of dynein in non-neuronal cells (19,20). In mammalian brain tissue dynein, dynactin and LIS1 can be coimmunoprecipitated (19,20) and genetic interactions of LIS1 with dynein, dynactin and microtubules have been suggested from studies of *Drosophila* (17,26). Furthermore, LIS1 colocalizes with dynein at the leading poles of neurons, perhaps serving to anchor dynein along the polarized microtubules of this region (27). Other cytoskeletal proteins that interact with LIS1 include NudC (28,29), cytoplasmic linker protein 170 (CLIP-170) (30), and tubulin (31,32). However, the molecular evidence for LIS1 interactions with microtubules has been confusing, as LIS1 has been shown to both stabilize microtubules *in vitro* in mammalian systems (31) and promote microtubule catastrophe in *A. nidulans* (32).

Although studies in fungi and cell culture have provided insights into the molecular mechanisms of LIS1 function, discerning the activity of this protein within the context of the mammalian brain remains paramount. In this regard, *Lis1* knockout mice provide insights required for understanding the anatomical and architectural milieu of LIS1-related neuronal migration (33,34). Homozygous *Lis1* null mutations are lethal in mice, wherein death ensues during early embryogenesis. Heterozygotes survive but exhibit evidence of delayed neuronal migration, as these animals display aberrant cortical neuron and radial glia morphology in the developing cortex.

Taken together, there are abundant data linking neuronal and nuclear migration defects with LIS1. However, the precise reasons why genetic disturbances associated with LIS1 cause human lissencephaly and its various medical consequences, such as mental retardation and epilepsy, are unknown. Specifically, ~90% of children with ILS and MDS display intractable epilepsy (35) (W.B. Dobyns, personal communication). Given the extreme complexity of the central nervous system, we contend that genetic analysis in a simple model organism may provide a complementary and rapid means toward discerning the functional role of LIS1 in neuronal development and activity.

Genetically tractable organisms that possess intact nervous systems represent a distinct advantage in addressing questions pertaining to these fundamental biological mechanisms. *C. elegans* is ideal in this regard, as this transparent microscopic nematode has a nervous system of precisely 302 neurons for which the complete neuronal connectivity has been defined (36). All major hallmarks of mammalian neurological function are conserved in *C. elegans*, including ion channels, axon guidance cues, receptors, transporters, synaptic components, and neurotransmitters [i.e. acetylcholine, dopamine, gamma-aminobutyric acid (GABA) serotonin] (37). Moreover, a rich history of previously isolated mutations, a wide variety of straightforward phenotypic assays for neuronal function and a plethora of GFP markers that highlight specific neuronal classes and processes are available for *C. elegans* research.

We previously performed an initial characterization of *C. elegans lis-1* gene expression that showed localization to several cell types in the worm, including proliferating cells and neurons. Additionally, the primary phenotype associated with LIS-1 depletion in *C. elegans* was embryonic lethality (18). In this work, we show that a *C. elegans lis-1* mutant is subject to seizure-like convulsions in the presence of a GABA antagonist. The cytological and molecular basis for these convulsions was investigated. We concluded that the *lis-1*-related convulsions observed did not result from improper migration of neuronal nuclei or axons, or from a nuclear division/apoptosis defect in *C. elegans* neurons. Rather, we have observed an apparent presynaptic defect wherein synaptic vesicles are improperly distributed throughout the GABAergic neuronal processes of *lis-1* mutant worms. Thus, mutation of *lis-1* in *C. elegans* may result in altered neurotransmitter function, possibly through defects in the microtubule cytoskeleton, as reduction in microtubule motor proteins and a synaptic vesicle-associated protein also resulted in similar neurological disturbances.

RESULTS

pnm-1(t1550) encodes a nonsense allele of *lis-1*

Several large-scale screens have been conducted to identify specific genes implicated in early embryonic cell division of *C. elegans.* The *pnm-1(t1550)* allele was initially isolated in one such screen, among a class of mutations that affect pronuclear movement within the one-cell embryo of *C. elegans* (38). Following fertilization of *pnm-1* homozygous mutant oocytes, migration and fusion of the sperm and egg pronuclei do not occur, whereas these processes do occur normally in heterozygous sibling embryos from *pnm-1* heterozygous hermaphrodites (and wild-type). This mutant phenotype is

indicative of errors involving pronuclear migration (pnm) and microtubule dynamics and results in embryos that undergo several rounds of spurious mitotic division before lethality occurs. This embryonic phenotype is also highly reminiscent of the nuclear migration defect observed with LIS-1 knockdown in *C. elegans* via RNA interference (RNAi) (18).

The *pnm-1* locus was predicted to genetically map near the region of linkage group III containing the *lis-1* gene (38). Therefore, rescue of the embryonic lethality phenotype in *pnm-1* homozygous embryos was performed via germline transformation of *pnm-1* heterozygous animals with the *lis-1* cDNA fused to the *pie-1* promoter, which is expressed in the early embryo (39). Worms heterozygous for *pnm-1* produce offspring with three different genotypes (+/+, *pnm-1*/+ and *pnm-1/pnm-1*). On the basis of Mendelian patterns of inheritance, ~25% of the total offspring should be *pnm-1* homozygotes. By examining the offspring from heterozygous hermaphrodites, which include all genotypic possibilities, 11% (139/1269) of the offspring have readily observable embryonic lethality characteristic of *pnm-1*/*pnm-1* offspring. Following rescue with the *lis-1* cDNA, observable embryonic lethality in the offspring decreased to 2% (19/947), representative of 83% embryonic rescue of *pnm-1*-based lethality.

To confirm the gene identity by direct sequencing, PCR was utilized to amplify the LIS-1 coding region from *pnm-1* homozygous worms (~30% of the *pnm-1* homozygotes are able to survive embryonic lethality). Sequencing of the *C. elegans lis-1* gene revealed a G to A transition at position 276 of the coding sequence that transformed a tryptophan to a stop codon. This nonsense mutation occurred at amino acid 92 (Fig. 1, diamond) at a residue that is highly conserved across species. Figure 1 shows an alignment of *C. elegans* and human LIS1 amino acid sequences and contains a collation of human patient mutation information such as splice-site mutations, nucleic acid lesions and amino acid substitutions (40,41). The worm mutation lies near known regions of homology to human LIS1 lesions that result in both nonsense and frame shift mutations (40,42). These combined sequencing, rescue and RNAi phenocopying data indicate that *pnm-1* is an allele of *lis-1* in *C. elegans.*

To further characterize postembryonic phenotypes in *pnm-1* animals that escape embryonic lethality, we examined *pnm-1* homozygous worms for generalized proliferative or developmental defects. Specifically, we examined the overall appearance, body size, and growth rate of the escaper animals and compared these characteristics with *unc-32* animals (the genetic background of the *pnm-1* strain). No obvious differences in viability, proliferation, size, or developmental timing were noted between the *pnm-1* homozygous ($n = 10$) and *unc-32* homozygous animals ($n = 10$) (data not shown). Both strains exhibit a pronounced lack of motility; this is a well-characterized phenotype associated with the *unc-32* mutation. The one notable difference between these two strains is in gonadal development, where *pnm-1*/*pnm-1* animals contain a disorganized gonad and subsequently are sterile, whereas *unc-32* animals have a normal gonad and are fertile. The sterility of *pnm-1* homozygotes corresponds to our previous results for *lis-1* knockdown by RNAi (18) and, to the best of our knowledge, does not impact any of the neuronal studies described herein. Thus, *pnm-1* homozygous mutant animals able to escape the embryonic division defects appear to develop into somatically normal animals.

Induction of convulsions in *pnm-1* worms

Approximately 30% of *pnm-1* homozygous animals are able to survive to adulthood. We sought to identify lissencephaly-like phenotypes associated with postembryonic *pnm-1* worms that escape lethality in early development. As many patients with lissencephaly experience epileptic seizures, our first avenue of inquiry was to determine if these animals had a propensity to display seizure-like convulsions. Induction of seizures or convulsions is readily achievable in many mammals with pentylenetetrazole (PTZ), a GABA antagonist (43). GABA is a widespread neurotransmitter in *C. elegans*, wherein the body wall muscle cells of this nematode are innervated by GABAergic inhibitory motorneurons, as well as cholinergic excitatory motorneurons. It is widely believed that PTZ treatment lowers an intrinsic threshold of GABA-related responsiveness in neurons, thereby revealing sensitized neuronal states that may be associated with either a genetic or physiological susceptibility to seizures.

Using digital video imaging, we captured the phenotypic effects of chemically inducing convulsions in a variety of *C. elegans* genetic backgrounds. The results of these convulsion assays are depicted in Figure 2. Wild-type N2 worms (0/300) do not experience PTZ-induced convulsions at concentrations of up to 20 mg/ml (data not shown); however, the highest concentration used in this study was 10 mg/ml PTZ (Fig. 2). The percentage of *pnm-1* homozygous animals undergoing convulsions was commensurate with PTZ concentration. At 1, 4, 6, 8 and 10 mg/ml PTZ the percentage of worms displaying convulsions is 48% (24/50), 80% (40/50), 78% (39/50) 84% (42/50) and 96% (48/50), respectively (Fig. 2). The *pnm-1* homozygous worms did not exhibit spontaneous seizures (0/50) during the experimental time frames of observation when PTZ was absent. As the genetic background of *pnm-1* animals contains a marker gene (*unc-32*) that encodes an allele of a vacuolar ATPase subunit that is targeted to synaptic vesicles of cholinergic neurons (44), we limited our study with *pnm-1* homozygous mutant worms to the effects on GABA neurotransmission. Importantly, *unc-32* animals did not exhibit convulsions when exposed to any concentration (1–10 mg/ml) of PTZ tested (0/300), nor do *pnm-1* heterozygous animals (0/300), as depicted in Figure 2.

PTZ-induced convulsions in *pnm-1* worms are best described as 'head-bobbing' convulsions, wherein the posterior half of the animal is essentially immobile whereas anterior muscle contractions occur repetitively. The convulsions are also characterized by a lack of pharyngeal pumping, an observation indicative of disrupted GABA neurotransmission, as the muscle cells on the pharynx contain GABA receptors. Still frames of *pnm-1* homozygous worms undergoing convulsions are shown at various time points in Figure 3A. The actual convulsions are quite striking and are best viewed as streaming video (25 frames/s) (Supplementary Material, Video 1). Additional videos, including an N2 control animal without PTZ (Supplementary Material, Video 2), and a

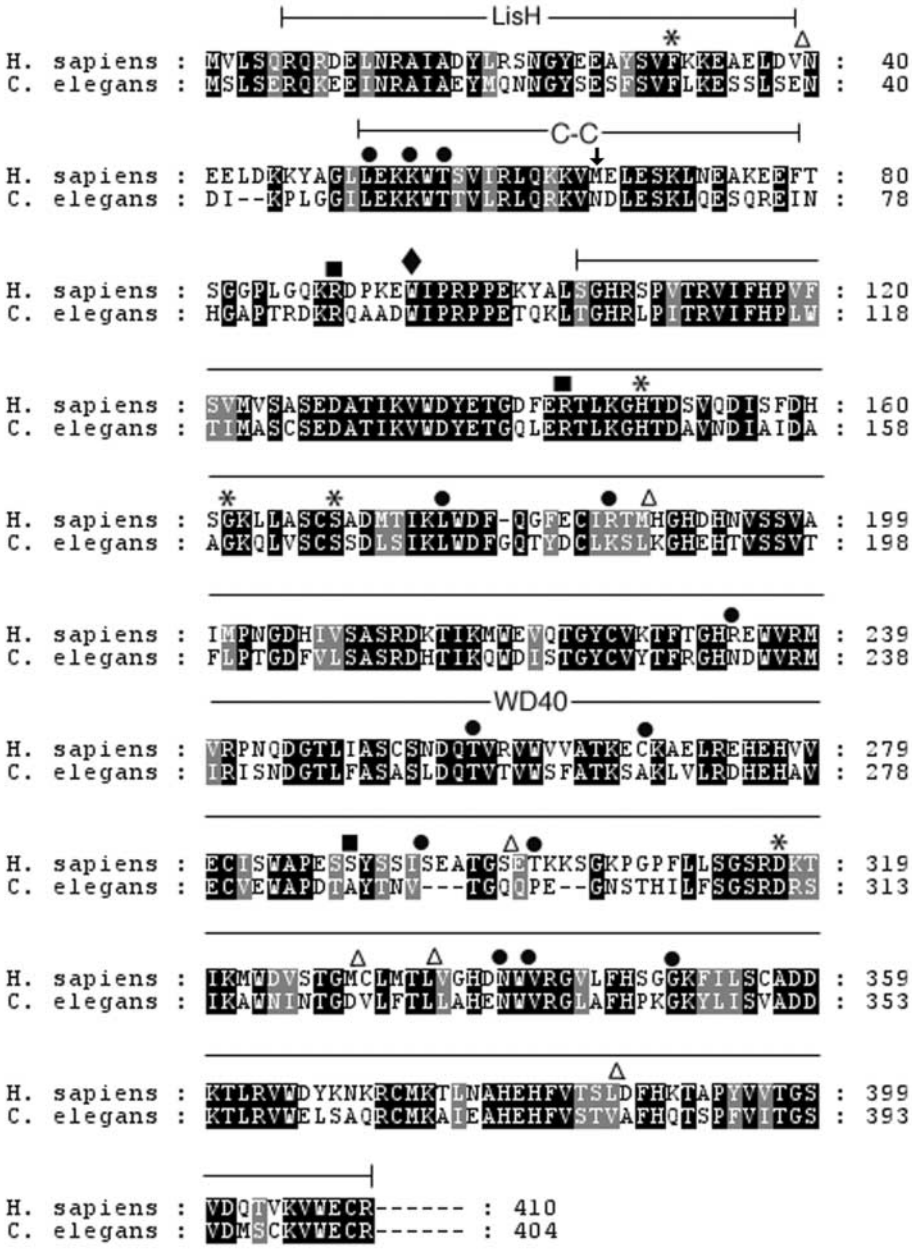

Figure 1. Amino acid sequence alignment between *C. elegans* and human LIS1 proteins. Residues shaded in black correspond to identical matches in sequence homology and residues shaded gray represent those with similar amino acid properties. The three main domains of the protein are indicated with brackets; the LIS1 homology domain (LisH) consists of residues 6–39, the coiled-coil domain (C-C) contains residues 51–79 and the seven WD40 repeat domains comprise residues 107–410 (96). The diamond represents the nonsense mutation identified in the *C. elegans lis-1* allele, *pnm-1(t1550)*. Additionally, known missense (asterisks), splice site (triangles), frame shift (circles) and nonsense mutations (squares) found in human intragenic mutations are denoted (40,41). An arrow designates the beginning of translation of the predicted gene product produced by the N-terminal deleted *Lis1* knockout mouse (34).

pnm-1 homozygous animal not exposed to PTZ (Supplementary Material, Video 3), are available for comparison.

Interestingly, PTZ-induced convulsions in *pnm-1* worms phenocopied convulsions displayed by multiple *C. elegans* GABA mutants exposed to this same GABA antagonist. Head-bobbing convulsions were observed in various GABA mutants including alleles of a GABA synthesis gene *unc-25(e156)*, GABA vesicular transporters *unc-46(e177)* and *unc-47(e307)* and the $GABA_A$ receptor *unc-49(e407)*. Previous research with these alleles has shown that they are strong mutations showing defects in all GABA-mediated behavioral functions (45,46,47). However, only *unc-49 (e407)* is a genetic null mutation (47). Still frames taken from streaming videos of a representative GABA mutant, *unc-25*, are depicted in Figure 3B and a corresponding video can be seen in the electronic supplemental material (Supplementary Material, Video 4). As with *pnm-1*, PTZ-induced convulsions in GABA mutants involve head bobbing only and are comparable to the

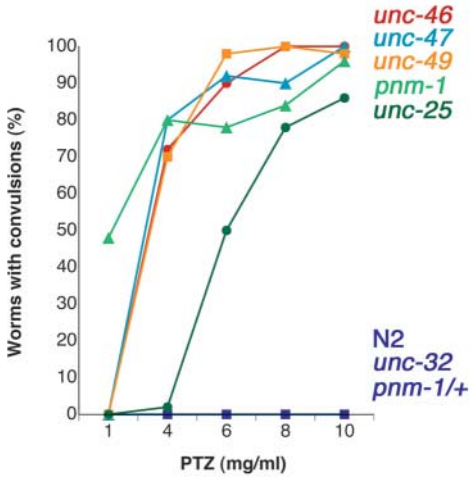

Figure 2. Dose–response curves for convulsions demonstrated in *C. elegans* mutants following exposure to increasing concentrations of PTZ. The response level (percent animals displaying convulsions/total sample size; $n = 50$) of various *C. elegans* strains is depicted for each concentration of PTZ ranging from 1 to 10 mg/ml. N2 wild-type worms, along with *unc-32* and *pnm-1/+* worms (collectively shown by dark blue squares), did not exhibit convulsions at any tested concentration of PTZ. *unc-46* (red circles), *unc-47* (light blue triangles), and *unc-49* worms (orange squares) containing mutations in GABA-related genes, all demonstrated very similar levels of convulsions at the concentrations of PTZ tested. *unc-25* animals (dark green circles) had fewer convulsions than other GABA mutants tested. *pnm-1* homozygous worms exhibited the greatest sensitivity of all worm strains assayed; 48% of these animals had convulsions in the presence of only 1 mg/ml PTZ (light green triangles).

convulsions demonstrated by *pnm-1* (Fig. 3A and B). All GABA mutants tested had convulsions at 10 mg/ml PTZ; *unc-25*, *unc-46*, *unc-47* and *unc-49* animals had 86% (43/50), 100% (50/50), 100% (50/50) and 98% (49/50) convulsions, respectively. This mirrors the 96% (48/50) convulsions demonstrated in *pnm-1* homozygous animals when exposed to the same concentration of PTZ (Fig. 2). None of the GABA mutant strains exhibited convulsions in the absence of PTZ.

The occurrence of convulsions in the *unc-49* strain (encoding a null allele of a GABA receptor) following exposure to PTZ raises a pharmacological question: how can a receptor null mutant respond to a chemical antagonist? Though *unc-49* encodes the best characterized and a highly conserved $GABA_A$ receptor in *C. elegans*, the completed genome sequence for this nematode reveals that additional receptor homologs with the potential to interact with PTZ also exist within the genome. These include another clear $GABA_A$ receptor homolog and numerous uncharacterized orphan receptors (E. Jorgensen, personal communication). Therefore, we postulate that the absence of the *unc-49* encoded receptor lowers a critical threshold, which PTZ then overcomes by acting upon additional, secondary receptors. This contrasts with the situation in wild-type worms, where the *unc-49* gene product remains fully functional, and in which PTZ has no effect at the concentrations used in our study.

The observation that GABA and *pnm-1* mutants share a similar convulsion phenotype was intriguing, especially because other mutations in genes important for neuronal function either do not result in a convulsion phenotype at all or yielded convulsions that are phenotypically distinct from those of *pnm-1* and GABA mutants. We looked for convulsions by testing several strains containing mutations in other neuronal genes, as examples of putatively unrelated gene products that may influence neuronal activity. For example, *unc-32* (the genetic background of *pnm-1*) is severely uncoordinated; it encodes an allele of a cholinergic vacuolar ATPase subunit. As noted earlier, when exposed to 10 mg/ml PTZ these animals do not display convulsions. We also tested *unc-4(e120)* worms, which contain a mutation in a homeodomain gene that is normally required for establishing the identity of the A class motor neurons DA and VA (48). The UNC-4 protein is required for movement, axon guidance and synapse formation; *unc-4* animals are incapable of moving backwards as a result of this mutation (49). However, despite the locomotory defect associated with this mutation, these animals do not have convulsions when exposed to PTZ (0/300; data not shown). We next examined *unc-43 (n498 n1186)* mutant worms. The *unc-43* worm encodes calcium/calmodulin-dependent serine/threonine kinase II (CaMKII), a Ca^{2+}-dependent protein kinase which is thought to be a general regulator of synaptic plasticity. *C. elegans unc-43* hypomorphs exhibit widespread hyperactivity in locomotion, egg laying and defecation (50). Additionally, *unc-43 (n498 n1186)* animals demonstrate a basal occurrence of spontaneous convulsions (J. H. Thomas, personal communication; 50). We observed that these animals experience full body convulsions in response to PTZ (100% at 10 mg/ml; $n = 50$), wherein these convulsions result from contraction of dorsal and ventral body wall muscles, followed by relaxation (Supplementary Material, Video 5). This is in contrast to the exclusively head-bobbing convulsions recorded for both *pnm-1* and GABA mutants. Still frames demonstrating *unc-43*-specific full body convulsions, in which the posterior, as well as the anterior, dynamically contract, are shown in Figure 3C.

Our results have illustrated an apparent GABA-specific phenotype, wherein mutations in *pnm-1* phenocopy the convulsions experienced by GABA mutants. Notably, these convulsions are distinct from mutations in other neuronally expressed genes. Indeed, some neuronal mutations do not respond with convulsions at all (*unc-32* and *unc-4*), whereas *unc-43* worms display convulsions phenotypically different from *pnm-1* and GABA mutants. Consequently, the shared and characteristic convulsion phenotype observed with both GABA and *lis-1* mutant worms prompted us to more closely investigate potential defects in GABA-related neurons in *pnm-1* worms, especially because GABA and LIS-1 are both expressed within the VD and DD motorneurons of the ventral nerve cord in *C. elegans.*

Neuronal division is normal in the ventral cord of *pnm-1* worms

Genetic mosaic analysis of *DLis1* in the developing *Drosophila* brain has demonstrated that underexpression of Lis1 can cause a reduction in the proliferation of neurons (51). Comparably, we have noted cell division defects in *C. elegans* mitotically dividing embryos when LIS-1 is reduced (18, this study). LIS-1 is also expressed in every motorneuron class of the ventral nerve cord in *C. elegans* (18, unpublished data). Taken together, we wanted to

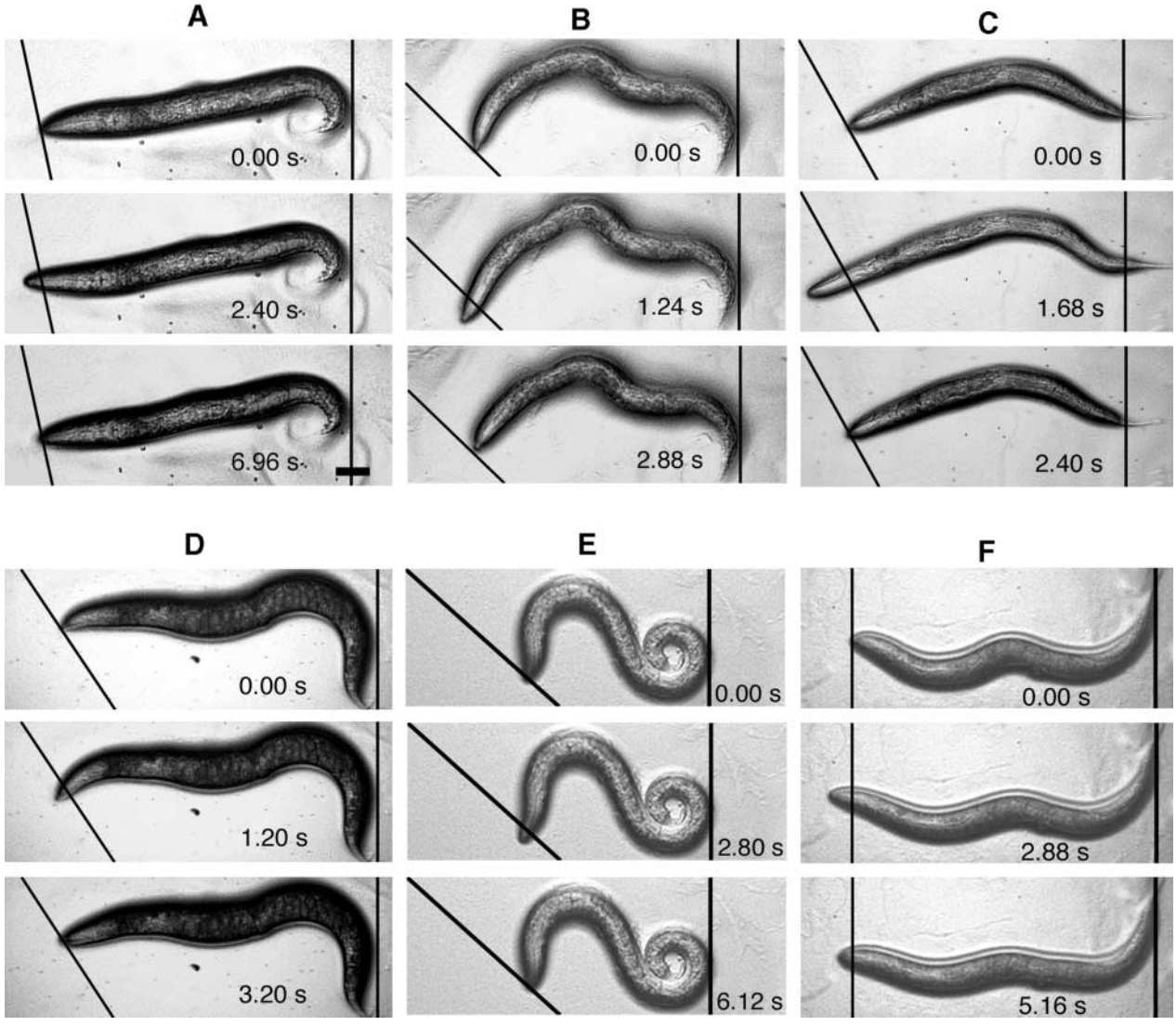

Figure 3. Still frame images demonstrating *C. elegans* strains undergoing convulsions following exposure to 10 mg/ml PTZ. The still images are representative frames selected from videos (25 frames/s) available in Supplementary Material. The black lines represent a stationary reference point for visualization of anterior and/or posterior movements in relation to time (indicated in s). Anterior is to the left in all images, where lines are placed perpendicular to the original position of the animal's nose. Note that *pnm-1* homozygous (**A**), *unc-25* (**B**), *dhc-1* (RNAi) (**D**), *unc-104* (**E**) and *snb-1* (**F**) animals display anterior-only movements of the head, whereas *unc-43* worms (**C**) display full body convulsions. Bar = 100 μm

determine if mitosis occurred normally within the ventral cord of *pnm-1* homozygous animals.

During *C. elegans* development, neurons within the ventral nerve cord must undergo several rounds of cell division, as well as apoptosis, in order for the appropriate number of neurons to be specified within the adult. For example, a newly hatched larva contains 22 motorneurons in the ventral cord and associated ganglia, whereas an adult animal has ~76 neurons (36). We examined the nuclei in the ventral cords of adult N2 and *pnm-1* homozygous animals to determine if *pnm-1* animals exhibited an abnormal number of nuclei within the ventral nerve cord or if the nuclei were unevenly spaced (possibly indicative of a nuclear migration defect). We determined that there was no difference between the number or spacing of nuclei (73 ± 3) between *pnm-1* homozygous worms ($n = 15$) and N2 worms ($n = 10$). Though we assayed neuronal cell division by 4′-6-diamidino-2-phenylindole (DAPI) staining adult animals, this is not sufficient to unequivocally conclude that the normal number of division events occurred during development. Although there is not a precedent for LIS-1 activity in apoptosis, aberrant proliferation in combination with a compensatory decrease in cell death could yield wild-type numbers of neuronal cell bodies as determined by our assay.

Neuronal migration and architecture in GABAergic neurons is normal in *pnm-1* worms

The hallmarks of human lissencephaly in brain morphology include the loss of normal gyral patterns within the cerebral

hemispheres and disorganization of the cerebral cortical cytoarchitecture resulting from abnormal migration of neurons during early brain development. At least a subset of these malfunctioning neurons express GABA (reviewed in 52). In *C. elegans*, the adult ventral nerve cord contains precisely 20 GABAergic motorneurons (45). As LIS-1 is expressed in all classes of neurons within the ventral nerve cord (18), GABA and LIS-1 are co-expressed in many of the same cells. Together with evidence indicating that *pnm-1* and GABA mutant worms share phenotypically similar convulsions, the coincident expression of GABA and LIS-1 in *C. elegans* further suggested the possibility that lissencephaly-related convulsions occur, at least in part, from disturbances in GABA neurons.

GABAergic neurons in *pnm-1* homozygous worms were analyzed for defective migration or architectural changes. An integrated GFP marker strain containing an *unc-47*::GFP transcriptional reporter construct, specifically highlighting the GABAergic neurons of *C. elegans*, facilitated this study (46). The *unc-47* gene is normally transcribed and expressed in all 26 GABAergic neurons of the worm, including the 20 ventral cord motorneurons (46). Within control animals, *unc-47*::GFP was localized in all GABAergic cell bodies and axons, as expected. This expression was strongest in the ventral cord and cell bodies, with slightly reduced expression in both the commissures and the dorsal cord (Fig. 4A, D and E). The *unc-47*::GFP strain was crossed into both the *pnm-1* and *unc-32* backgrounds to determine whether *pnm-1* worms displayed any defects in overall neuronal architecture. GABAergic neurons were rigorously examined for any defects in the extension of axons and for branching defects of the commissures. We did not find any discernable expression pattern differences between either *unc-47*::GFP alone ($n = 50$), *unc-47*::GFP; *unc-32* control animals ($n = 50$) (image not shown) or *unc-47*::GFP; *pnm-1* animals ($n = 50$) at the light microscope level (Fig. 4B). The results of this analysis are compiled in Table 1. We concluded that this *pnm-1* mutant allele of *lis-1* does not affect overt GABAergic neuronal architecture.

Within the *C. elegans* field, neuronal migration is commonly studied by visualizing the two HSN cells (hermaphrodite-specific neurons required for egg laying), as well as two cells arising from the Q-neuroblast lineage, AVM and PVM, which are touch sensory neurons. We examined neuronal migration following introduction of the *pnm-1* mutation into transgenic lines expressing GFP in the appropriate cell types; this facilitated examination of alternative neuronal migration defects that would not be observed by our other assays. To examine HSN migration, we crossed the *pnm-1* strain with worms expressing a GFP transgene that is expressed within the HSN neurons. Specifically, we utilized a strain containing the arrestin promoter fused to GFP (arrestin::GFP); arrestin is a cytosolic protein involved in G protein-coupled receptor desensitization that is expressed in many neurons within the worm but shows particularly clear GFP expression within the two HSN cells. We did not observe any obvious migration defects in the final position of the HSN neurons when analyzed within the *pnm-1* or *unc-32* backgrounds ($n = 50$ for each strain; data not shown). In order to examine the Q-neuroblast lineage, the final position

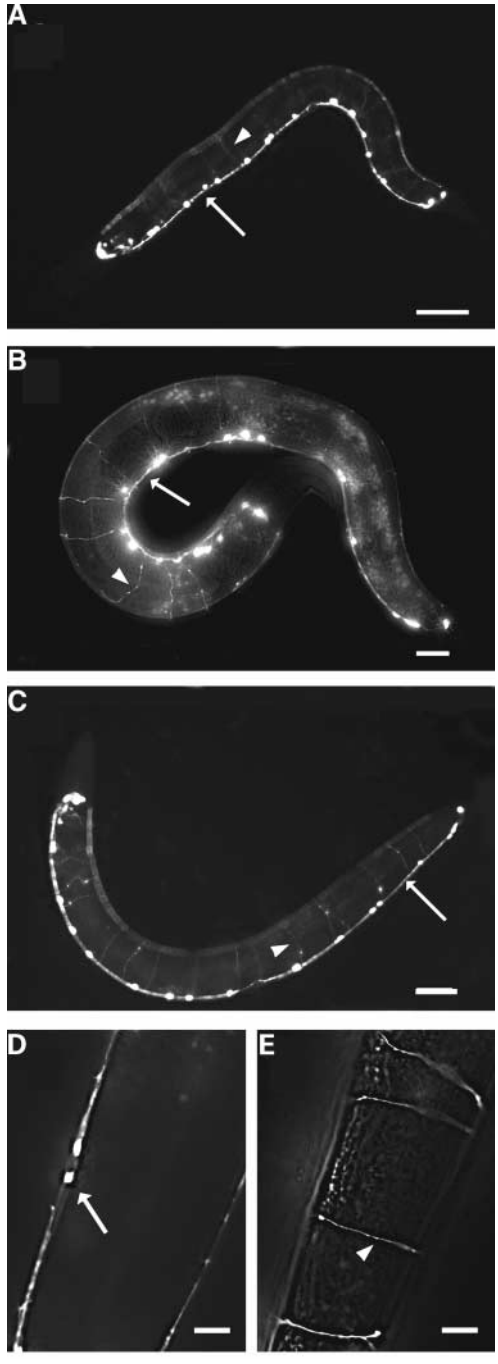

Figure 4. GABAergic neuron architecture is unaffected by *pnm-1* or *dhc-1* (RNAi). A transcriptional reporter gene fusion, *unc-47*::GFP, reveals the neuronal cell bodies and processes of GABAergic neurons and commissures in *C. elegans* [**A**; *lin-15(n765ts) oxIs12 X* (integrated strain carrying *unc-47*::GFP)]. One focal plane is shown for each strain, inclusive of representative commissures and processes (anterior is to the left in all images). Arrows point to tightly fasciculated ventral nerve cords in all strains; arrowheads demonstrate wild-type commissures extending from ventral to dorsal nerve cords. Introduction of the *lis-1* mutation associated with the *pnm-1(t1550)* allele by genetic crosses with *unc-47*::GFP [**B**; *lin-15(n765ts) oxIs12 X; pnm-1(t1550)*] or reduction of DHC-1 levels by RNAi [**C**; *lin-15(n765ts) oxIs12 X* fed *dhc-1* dsRNA] does not result in any discernable change in the overall architecture of the GABAergic system. Bar = 100 μm. (**D**) and (**E**) High magnification views of the ventral cord (D) and commissures (E) exhibiting normal GABA neuron architecture, as illuminated by the *unc-47*::GFP reporter. Bar = 350 μm.

Table 1. Alterations in LIS-1 or DHC-1 do not cause changes in GABAergic architecture

Worm strain	Genotype	Wild-type expression[a] (%)	Axonal extension defects (%)	Branched commissures (%)
unc-47::GFP	*lin-15(n765ts) oxIs12 X* ($n = 50$)	96	0	4
unc-47::GFP; *unc-32*	*lin-15(n765ts) oxIs12 X* ($n = 50$)	100	0	0
unc-47::GFP; *pnm-1*	*lin-15(n765ts) oxIs12 X;pnm-1(t1550)* ($n = 50$)	98	2	0
unc-47::GFP + *dhc-1* (RNAi)	*lin-15(n765ts) oxIs12 X* fed *dhc-1* dsRNA ($n = 100$)	97[b]	2	1

[a]See Figure 4, where arrows point to tightly fasciculated ventral nerve cords in all strains; arrowheads demonstrate wild-type commissures extending from ventral to dorsal nerve cords.
[b]A total of 82% of the ventral cords in these animals appeared completely wild-type; however, 15% appeared wild-type with respect to axon extension and commissures but lacked wild-type character with respect to muscular attachment.

of the AVM and PVM touch neurons was assayed by crossing a strain carrying the *mec-17* promoter fused to GFP (*mec-17* is expressed in these touch neurons) (53) with the *pnm-1* and *unc-32* strains. There was no deviation from the wild-type expression pattern for the AVM and PVM neurons ($n = 50$ for each cross; data not shown). Therefore, as was also observed for GABA neurons, the *pnm-1* mutation does not affect neuronal migration of HSN or Q-neuroblast cells.

The distribution of synaptic vesicles is disrupted in GABA neurons of *pnm-1* worms

As the neuronal architecture appeared normal in GABAergic neurons, the distribution of GABAergic synaptic vesicles was examined in the *pnm-1* homozygous mutant background. Specifically, transgenic worms containing a fusion protein construct were used that allows for visualization of GABA vesicles. This construct consists of the synaptic vesicle-associated membrane protein synaptobrevin (SNB-1) fused to GFP and is expressed under the control of an *unc-25* GABA-specific promoter (54). Animals carrying an integrated array of *unc-25*::SNB-1::GFP were crossed into *pnm-1* mutant animals and the distribution of GABA specializations was visualized. In control animals (both wild-type and *unc-32*, $n = 74$ for each strain), the GFP fluorescent signal was visualized as discrete puncta dispersed evenly along the ventral nerve cord in positions consistent with the pattern of VD motorneuron synaptic output (Fig. 5A and B). These puncta were similar to the distribution of wild-type GABAergic neuromuscular junctions identified via EM analysis (36,55,56). Notably, in 22% ($n = 74$) of the *pnm-1* homozygous animals, the synaptic vesicle puncta appear significantly altered from control animals (Table 2). The most common differences observed were in regions along the ventral cord that contained gaps without GFP puncta (19%) and irregularly sized and unevenly spaced puncta (3%; Fig. 5C). As each punctum likely represents a synaptic terminal, these gaps indicate a defect in vesicle transport within GABAergic neurons. Although fewer animals had observable vesicle/synaptic gaps when compared with convulsion rates (e.g., 22% synaptic defects versus 48% convulsions at 1 mg/ml PTZ for *pnm-1* animals), it is important to remember that these synaptic gaps were analyzed in live animals and, presumably, are dynamically changing in response to stimuli. Furthermore, it is possible that additional animals have subtle synaptic defects unresolved at the light microscope level.

To determine whether the observed vesicle transport defect within *pnm-1* worms is occurring pre- or postsynaptically, *pnm-1* worms were tested for sensitivity to the GABA agonist muscimol. If a defect is presynaptic, then muscimol causes body muscle paralysis owing to the inhibition of postsynaptic GABA function (45). Upon exposure to muscimol, 100% of the *pnm-1* animals ($n = 20$) responded with paralysis, as did 100% of the presynaptic GABA mutants tested (*unc-25*, *unc-46* and *unc-47*; $n = 20$ for each strain). Conversely, 0% of the *unc-49* animals ($n = 20$), containing a mutation defective in postsynaptic GABA reception, were paralyzed by muscimol at the concentration tested. These results indicate that the GABA transmission defect in *pnm-1* is likely occurring presynaptically.

Aberrant molecular motor protein function also causes GABA transmission defects

Studies with *A. nidulans* and mammalian cells have shown that LIS1 physically interacts with cytoplasmic dynein heavy chain and likely serves as a functional regulator of motor activity (25,57,58). Therefore, we wanted to determine whether a dynein mutant also had altered GABA vesicle defects similar to those observed in *pnm-1* mutants of *C. elegans.* Unfortunately, viable mutations in the *dhc-1* gene, encoding dynein heavy chain protein (DHC-1), were not available and depletion of *dhc-1* by microinjection of dsRNA is lethal (59). Therefore, to obtain non-lethal *dhc-1* phenotypes, the technique of bacterial dsRNA feeding to evoke RNAi was employed. This method was carefully titrated to bypass lethality, as much weaker phenotypes can be obtained by modulating the potency of RNAi in *C. elegans* (60).

To investigate whether *dhc-1* (RNAi) worms phenocopy the neurological defects observed with *pnm-1* animals, worms containing the *unc-25*::SNB-1::GFP transgene were exposed to dsRNA targeting *dhc-1.* We determined that the normal distribution of GABA vesicles was clearly disrupted in these worms (Fig. 5D). Notably, as observed within the GABAergic neurons of *pnm-1* homozygous worms, 29% of *dhc-1* (RNAi) worms ($n = 100$) had regions with gaps in the GFP pattern (Table 2). Muscimol assays revealed that the defect was presynaptic in the *dhc-1* (RNAi) animals, as these animals responded with total paralysis. To ensure that the altered

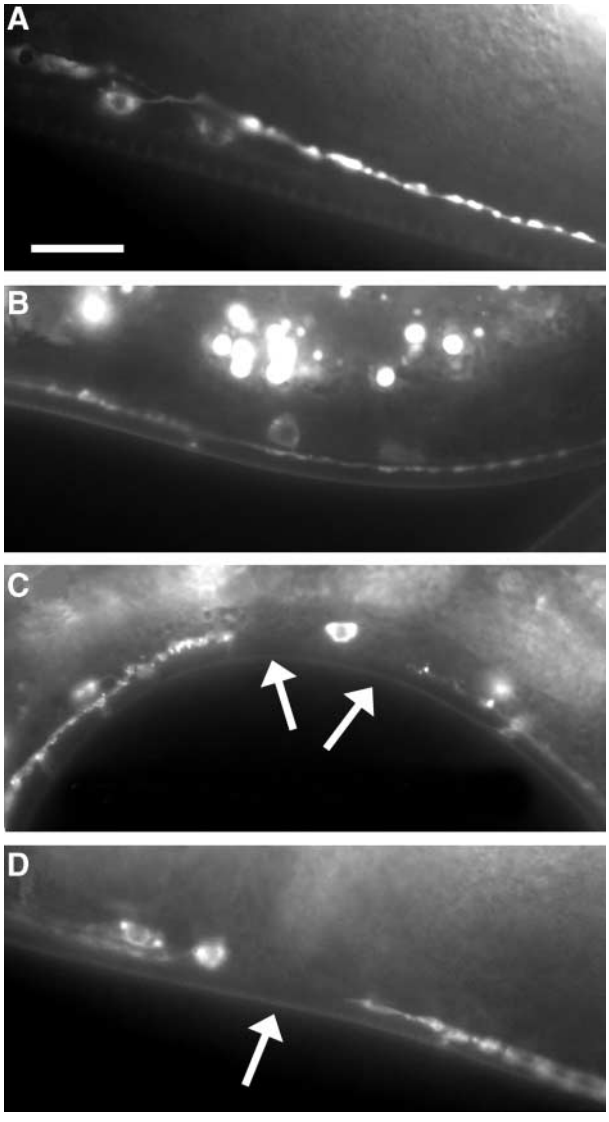

Figure 5. Changes in GABA synaptic vesicle distribution following alterations in LIS-1 or DHC-1. As shown in (**A**) and (**B**), *unc-25*::SNB-1::GFP is localized to discrete puncta along the ventral nerve cord consistent with the normal motorneuron pattern of synaptic output in both the wild-type [A; *lin-15(n765ts) X juIs1*] or *unc-32* [B; *lin-15(n765ts) X juIs1*] background. Round spots are autofluorescent gut granules that are not associated with GFP expression. In contrast, introduction of the *lis1* mutation associated with the *pnm-1(t1550)* allele by genetic crosses with *unc-25*::SNB-1::GFP worms leads to the appearance of regions lacking GFP fluorescence (arrows) within the ventral cord [**C**; *lin-15(n765ts) X juIs1; pnm-1(t1550)*]. This result is mimicked by reduction of DHC-1 levels by RNAi [**D**; *lin-15(n765ts) X juIs1* fed *dhc-1* dsRNA]. All images were taken of the region just posterior to the vulval opening. Bar = 5 μm

GABA vesicle distribution was not simply a problem with the GABAergic neuronal architecture, *unc-47*::GFP worms were also fed dsRNA versus *dhc-1* and examined for defects. As shown in Table 1, 97% ($n = 100$) of the *dhc-1* (RNAi) worms possessed intact axon extensions and commissures in GABAergic neurons (Fig. 4C). The general effectiveness of RNAi in GABA neurons was judged using control dsRNA targeting GFP. In 98% of all animals tested ($n = 100$) *unc-25*::SNB-1::GFP knockdown was achieved by RNAi feeding in simultaneously performed trials (data not shown). Neuronal cell division was also assayed; both the spacing and number of nuclei visualized by DAPI staining were comparable to wild-type levels (73 ± 3; $n = 10$).

For assessment of the convulsion phenotype, N2 animals fed dsRNA targeting *dhc-1* were exposed to 10 mg/ml PTZ. Notably, 44% (22/50) of these *dhc-1* (RNAi) animals were immobilized at the posterior and displayed weak head-bobbing convulsions, similar to both *pnm-1* and GABA mutants (Fig. 3D), although not as visibly dramatic (Supplementary Material, Video 6). Many *dhc-1* (RNAi) animals appeared to have a more generally stiff or 'tonic' appearance in the presence of PTZ, whereas control *dhc-1* (RNAi) animals, in the absence of GABA antagonist, displayed normal locomotion and foraging behavior. These results correlate with *lis-1* (RNAi) experiments, wherein wild-type N2 RNAi-treated worms display a tonic phenotype when exposed to PTZ as well (data not shown). The distinction between the *lis-1* (RNAi) and *pnm-1* convulsion phenotype may be due to the inherent difference between partial knockdown of an entire protein versus expression of a genetic mutation, respectively. These combined data suggest a common activity for LIS-1 and dynein within neurons wherein the observed convulsion phenotype is a functional consequence of aberrant expression.

Dynein is involved in numerous microtubule-based cellular processes, one of which is a clearly defined role in retrograde transport. In support of this, *C. elegans* researchers have very recently reported the isolation of one allele of dynein light intermediate chain (*dli-1*) and two alleles of dynein heavy chain (*dhc-1*) from a genetic screen designed to identify mutations that misaccumulate synaptobrevin (61). As synaptobrevin is considered a reporter for axonal transport, this result is most significant in light of our own data indicating that GABA vesicles are mislocalized in both cytoplasmic dynein and *lis-1* mutant backgrounds. This report also determined that UNC-104, a neuronal-specific kinesin-like protein, requires the dynein motor for transport (61).

UNC-104 is homologous to the human axonal transporter of synaptic vesicles, KIF1A, and is required for anterograde axonal transport of synaptic vesicles in *C. elegans* (62). EM analyses of *unc-104* worms have provided evidence that these animals do not have densely packed neurotransmitter vesicles near the active zone in neurons of the ventral cord (63). Instead, small vesicles were clustered together in neuronal cell bodies. Additionally, it was shown that the presence of SNB-1::GFP is primarily visualized in the cell body of neurons and not within the synaptic regions of neurons of *unc-104* animals (54). To further investigate the possibility that defects in neuronal vesicle trafficking can lead to convulsions, we examined a worm strain containing an *unc-104* mutation [*unc-104 (e1265)*] for PTZ-induced convulsions. Upon exposure to 10 mg/ml PTZ, 48% (24/50) of the worms presented a tonic posture with mild head-bobbing convulsions as shown in Figure 3E and Supplementary Material, Video 7. These convulsions were similar to those displayed by *dhc-1* (RNAi) animals. Without the presence of PTZ, *unc-104* worms maintained their characteristic Unc phenotype but did not have convulsions (0/50), nor were they tonic in appearance

Table 2. Alterations in LIS-1 or DHC-1 result in a change in GABAergic synaptic vesicle localization

Worm strain	Genotype	Wild-type expression (%)	Gaps in GFP (%)	Bunched GFP (%)
unc-25::SNB::GFP	*lin-15(n765ts) X juIs 1* ($n = 74$)	92	8	0
unc-25::SNB::GFP;*unc-32*	*lin-15(n765ts) X juIs1;unc-32(e189)* ($n = 74$)	93	7	0
unc-25::SNB::GFP;*pnm-1*	*lin-15(n765ts) X juIs1;pnm-1(t1550)* ($n = 74$)	78	19	3
unc-25::SNB::GFP+ *dhc-1* (RNAi)	*lin-15(n765ts) X juIs1* fed *dhc-1* dsRNA ($n = 100$)	71	29	0

(Supplementary Material, Video 8). Previous work at the EM-level has shown that although synaptic vesicle transmission defects in the *unc-104* ventral cord are evident, axonal outgrowth is normal in these animals (63). Thus, *unc-104* is another example of a strain that has neurotransmitter trafficking defects and also displays convulsions.

Synaptic transmission defects are associated with convulsions when exposed to PTZ

Although these data lend support for a neurotransmitter trafficking mechanism being responsible for the convulsion phenotype, they do not fully prove that defects of synaptic transmission are involved. As dynein mutants in *C. elegans* can cause a misaccumulation of the vesicle associated protein synaptobrevin (61), we examined a hypomorphic worm strain carrying a synaptobrevin mutation, *snb-1(md247)*, for convulsions. These worms have a variety of behavioral phenotypes that are consistent with an overall reduction in synaptic transmission. Furthermore, electrical activity assays have provided additional proof that SNB-1 is required for synaptic transmission (64). Therefore, if exposure of *snb-1* worms to PTZ were to cause convulsions, it would corroborate our data indicating that synaptic transmission defects can lead to this phenotype. Upon exposure to 10 mg/ml PTZ, *snb-1* worms did indeed have convulsions (but not in the absence of PTZ). In fact, 98% (49/50) of the animals exhibited a tonic posture and mild head-bobbing convulsions that are reminiscent of those observed with *pnm-1*, GABA and motor protein mutants (Fig. 3F and Supplementary Material, Video 9). These data lend support to our hypothesis that neurotransmitter trafficking defects, such as those incurred by defective motor proteins or vesicle components, contribute to a possible mechanism accounting for the observed *pnm-1* convulsions. This, in turn, allows us to postulate that the epilepsy experienced by lissencephalic patients may be a consequence of a synaptic transmission defect rather than purely a result of abnormalities within the organization of the cerebral cortex.

DISCUSSION

Significant advances have been made toward an understanding of normal neuronal migration and the cortical malformations that stem from genetic deficits in this mechanism. The identification of the *LIS1* gene as causative in classical lissencephaly has led to correlative studies between cortical defects and biochemical effectors of LIS1 (3,9). This discovery has opened the door to the application of powerful comparative genomic analyses in simple genetic model systems designed to rapidly discern the evolutionarily conserved intricacies of LIS1 function.

Although almost all patients with lissencephaly, including those with ILS and MDS, suffer from epilepsy, the role of the cortical malformation *per se*, and the role of the causative gene, such as *LIS1*, in this aspect of syndrome remains unresolved. Though prospective studies have not been done, medical experience has shown that the epilepsy in patients with lissencephaly clearly worsens over time, and worsens the overall severity of the disease (40,65) (W.B. Dobyns, personal communication). Further, the epilepsy associated with LIS1 mutations is typically more severe than associated with mutations in doublecortin (*DCX*), a gene implicated in X-linked lissencephaly. LIS1 expression persists through the postnatal and adult brain whereas DCX does not, so that impairment of other LIS1 functions such as regulation of vesicular transport may contribute to the epileptic phenotype (W.B. Dobyns, personal communication). Furthermore, a direct link between LIS1 and epileptic seizures in animal models has been demonstrated. Following kainic acid-induced seizures in rats, there is an immediate reduction in LIS1 protein levels (66). This suggests that the reduction of LIS1 levels in lissencephalic patients may lower LIS1 activity below a critical level, thereby predisposing these patients to seizures. Supporting these conclusions, there is a correlation between LIS1 reduction in heterozygous knockout mice and an increased occurrence of seizures (33,34). Despite these advances, the cytological consequences of decreased levels of LIS1 protein activity remain unclear.

It remains possible that disrupted cell positions within the lissencephalic brain may not be wholly responsible for lissencephaly-related epilepsy. Instead, it has been suggested that intrinsic properties of the neurons may be causative (67). This hypothesis is bolstered by evidence gathered from the *reeler* mouse, in which a mutant extracellular matrix molecule is produced, leading to cortical malformations that are not as correlative with the occurrence of seizures as are LIS1 mutations (67). In contrast, the LIS1 protein interacts with many components of the neuronal cytoskeleton. Disruption of microtubules, actin and associated motor proteins could dramatically alter normal neuron function and influence the activity of neurotransmitter receptors and ion channels. In this regard, we explored the relationship between LIS-1 cytoskeletal function and convulsions in *C. elegans.*

Surprisingly, no overt defects in the overall GABAergic neuronal architecture were observed at the light microscope level in *pnm-1* worms encoding a defective LIS-1 protein. However, this does not preclude the possibility that electron microscopy analysis would reveal more subtle subcellular

neuronal defects in microtubule structure. For example, previous analyses of worms containing mutations in two mechanosensory genes, *mec-7* and *mec-12*, revealed EM-level defects of microtubule structure (68). These microtubule defects were not apparent at the light microscope level and, in fact, the affected neurons appeared normal. Unlike mechanosensory mutants, the limited viability and sterility of *pnm-1* homozygotes renders these animals very problematic for ultrastructural analyses. However, the advent of GFP reporter technology has allowed for illumination of other cellular consequences of neuronal malfunction, as we have observed using a fluorescent synaptic vesicle marker. Another interesting possibility for the absence of overt neuronal migration defects in *pnm-1* animals is that the physical distances traveled by migrating neurons in the human brain are many times those of microscopic worms (in which an entire adult animal is $\sim$1 mm long). Thus, the biophysical and cellular constraints imposed by LIS1 mutations might have different consequences in different species.

In both humans and worms, epileptic-like convulsions can result from a multitude of factors. Some or all of the following could be altered: neurotransmitter release, receptor levels, synapses, membrane potentials, neuronal differentiation or cytoskeletal function (67). Neurons require transport of organelles, vesicles, cytoskeletal proteins and signaling proteins for proper function. Evidence from *Drosophila* indicated that reduced expression of *Lis1* results not only in less dendritic branching, but also caused defective axonal transport (51). We have determined that the distribution of GABAergic synaptic vesicles along the ventral cord within *pnm-1* mutant worms is abnormal. Findings of similar neurological phenotypes following mutation or depletion of cytoplasmic dynein heavy chain, a protein known to interact with LIS1, add further support to this scenario (61; this study). We contend that the presence of synaptic defects, along with PTZ-induced convulsions, within both *pnm-1* and *dhc-1* (RNAi) worms, is at least partially indicative of cytoskeletal deficiencies within the GABAergic neurons of *C. elegans.* There is recent precedent for cytoskeletal involvement in neurological disease; cytoplasmic dynein and dynactin dysfunction have been shown to cause exclusively neuronal defects in human motor neuron disease (69,70).

Cytoplasmic dynein and LIS1, along with dynactin, CLIP-170, EB1, adenomatous polyposis coli (APC) and CLASPs, are all considered to be 'plus-end-tracking proteins' that localize to the plus ends of microtubules (reviewed in 71). The plus-end localized dynein/dynactin complex may serve as a cargo loading site on microtubules, as has been suggested from studies of mammalian cells and fungi (72–76). It has been demonstrated that *A. nidulans nudF* mutants (the *lis-1* homolog) accumulate dynein and dynactin at plus ends, suggesting that LIS1 may facilitate dynein movement toward the minus end of microtubules (76).

Dynein is also responsible for retrograde vesicle transport along microtubules within neurons. *Drosophila* strains with mutations in cytoplasmic heavy or light chain or dynactin component $p150^{Glued}$ show defects in the transport of synaptic vesicle components within neuronal axons (77). LIS1 physically interacts with two regions of dynein, both the cargo-binding region and the first AAA (ATPases Associated with cellular Activities) repeat of this motor protein (58). Furthermore, as LIS1 and CLIP-170 have been shown to interact, LIS1 may function as an adaptor protein coordinating dynein activity and cargo binding (30). In neurons, this could involve mediating the proper interaction between dynein and GABA- or VGAT-containing vesicles for recycling or reuse. A defect in retrograde transport of GABA vesicles from the presynaptic cleft back toward the nucleus could lead to a decrease in the available presynaptic GABA pool. A decrease in synaptic GABA would, in turn, result in a loss of GABAergic muscular inhibition and hyperexcitation.

Additionally, while dynein is not conventionally thought to have a role in anterograde fast transport, several studies have reported a link between plus-end- and minus-end-directed motors that suggest an interdependency of function exists (61,78,79,80,81). Kinesin was demonstrated to be required for the accumulation of cytoplasmic dynein and dynactin at microtubule plus ends in *A. nidulans* (75). Blocking the interaction of dynein and dynactin in extruded squid axoplasm resulted in a bidirectional block in vesicle transport along microtubules (81). Likewise, genetic studies in *Drosophila* have shown interactions between dynein and dynactin that can result in a bidirectional inhibition of axonal transport (77). Recent work in *C. elegans* lends support to this by showing that mutations in cytoplasmic dynein components cause misaccumulation of synaptobrevin, a protein that is dependent on functional anterograde transport by kinesin (61). When considering that LIS-1 interacts with dynein, *pnm-1* mutant animals may also have deficient retrograde and anterograde transport of GABA along microtubules (Fig. 6). Thus, molecular motors and associated proteins involved in the transport of neurotransmitters may very well play a causative role in some forms of epilepsy.

This is the first report that correlates defects within the *lis-1* gene with vesicle trafficking deficiencies. Synaptic vesicle transmission has been linked with seizures in human patients. For example, the synaptic vesicle protein synapsin I, which is involved in neurotransmitter release, has been identified as the causative mutation in a familial form of X-linked epilepsy (82). Additionally, mice deficient for synapsin I also exhibit seizures that are correlated with synaptic vesicle clustering defects (83). Our data show that a hypomorphic mutation in synaptobrevin also causes convulsions and is linked to synaptic vesicle clustering. Whereas these are examples of synaptic exocytosis defects, mutations affecting endocytosis have also been linked to seizures. Amphiphysins belong to a protein family involved in clathrin-mediated endocytosis of synaptic vesicles. Depletion of amphiphysin 1 results in synaptic vesicle recycling defects and rare, irreversible seizures (84). CLIP-170 has also been determined to have a role in retrograde endosome trafficking via endosome–microtubule interactions (85). Furthermore, studies have implicated dynein motor complex function in retrograde endosomal trafficking (73,86). For example, disruption of the dynactin–dynein complex in COS7 cells by overexpression of dynamitin led to dispersion of endosomes toward the cell periphery (86). It has been recently demonstrated that the ClC-2 ion channel interacts with the dynein motor complex *in vivo* and *in vitro* (87), supporting the putative role for the dynein complex in retrograde endosome trafficking. Mutations in ClC-2 have

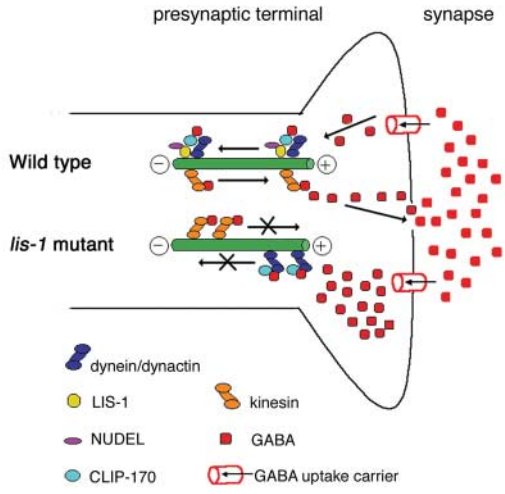

Figure 6. A model depicting a potential role for LIS1 in mediating cytoskeletal interactions necessary for GABA neurotransmission. LIS1 may be involved in coordinating dynein motor activity in binding and transporting GABA (or VGAT-containing) vesicles at the plus ends of microtubules. A defect in LIS1 or dynein function could result in a failure of retrograde transport from the presynaptic cleft toward the nucleus for recycling or reuse, leading to the observed aberrant distribution of GABA vesicles at synaptic junctions. Additionally, the putative interdependency of function between plus-end- and minus-end-directed motors could contribute to deficient exocytosis of GABA via an inhibition of kinesin-based anterograde transport resulting from defects in dynein motor function.

also been linked to inherited forms of idiopathic generalized epilepsy (IGE) where these altered channels are expected to lower the transmembrane chloride gradient essential for GABAergic inhibition (88).

Although we cannot rule out the possibility that the convulsions we have observed within the *pnm-1* mutant animals are a result of defects in local endosome recycling, our data are most consistent with a model wherein convulsions are caused by failure in vesicle trafficking. Synaptic vesicles and their neurotransmitter cargo must travel from the site of docking at the membrane of the presynaptic cell before they can enter the endosomal pathway. Only after vesicles travel from the cell surface via microtubule system do they enter the endosomal recycling pathway. In the presence of the GABA antagonist PTZ, aberrant expression of dynein, kinesin, or synaptobrevin results in mild head-bobbing convulsions, a phenotype that is reminiscent of the convulsions seen with mutations in GABA transmisson and *lis-1*. This phenotype is coincident with observable synaptic defects in vesicle distribution within the *C. elegans* ventral nerve cord of these mutants. Taken together, these data correlate with a hypothesis that vesicle trafficking defects may contribute to convulsive phenotypes, such as those experienced by lissencephaly patients.

The convulsion phenotype we observed in most worm strains responsive to PTZ consisted of anterior head bobbing and posterior immobilization. Notably, cytoskeletal and GABA-related mutant strains mimicked this phenotype. In contrast, other neuronal worm mutants either did not respond to PTZ (*unc-4* or *unc-32*) or responded with a phenotypically different type of convulsion (*unc-43*). The differential susceptibility of *unc-43* mutants to PTZ treatment is a probable result of the documented inherent hyperexcitability of these specific CaM kinase II defective animals (50). Nevertheless, mutations in PTZ-responsive motor proteins or associated components, kinesin (UNC-104/KIF1A), cytoplasmic dynein heavy chain and LIS1, clearly affect more cellular processes than simply GABA transmission. Likewise, SNB-1, a vesicle-associated protein, is involved in generalized neurotransmission. Therefore, the apparent specificity of the convulsion phenotype observed is likely due to our use of PTZ, a GABA antagonist, for these studies. We speculate that the use of chemical inducers designed at disrupting other neurotransmission pathways may yield their own distinct convulsive phenotypes and this represents a most interesting direction for future investigation. However, we limited our studies to the GABAergic system because the genetic background of the *pnm-1* strain (*unc-32*) encodes a tightly linked allele of a vacuolar ATPase subunit specific to cholinergic neurons, thereby precluding an analysis of the cholinergic system with the *pnm-1* mutation. Continued mutational analyses in *C. elegans* via the isolation of weak *lis-1* alleles, not linked to known neuronal mutations, could provide significant insights into the broader impact of LIS-1 malfunction on neuronal activity.

LIS1 is highly expressed in the Cajal-Retzius cells of human brains, neurons that produce high levels of GABA (52,89). Although the mechanisms connecting GABA with epilepsy are yet to be elucidated, altered GABA transmission has been linked with seizures (reviewed in 90). Rescuing the convulsion phenotype using a GABA-specific promoter to drive *lis-1* expression within GABA neurons of *C. elegans* could strengthen an association between GABA and *lis-1*. However, phenotypic rescue in neurons is particularly tricky; it has been shown that even a small decrease in cortical GABAergic inhibition can promote epileptogenic activity (91). In this regard, an attempt at neuronal rescue of *pnm-1* was unsuccessful using an *unc-47* (GABA transporter) promoter driving *lis-1* (data not shown). It is very likely that the *unc-47* promoter does not initiate *lis-1* expression at an appropriate stage in development, prior to synaptogenesis. As a predisposition to seizures involves factors that perturb the balance between GABA inhibition and neuronal excitation, an association between GABA and LIS-1 remains plausible.

Comprehensive analysis of the mechanisms by which LIS1 acts will likely elucidate regulatory factors governing the cytoskeletal control of neuronal development and activity. Although use of a non-mammalian model system renders it impossible to fully recapitulate the expected complexities of cortical malformations, it is advantageous for discerning molecular subtleties of cellular dysfunction associated with specific genetic deficits. In this regard, we have shown with *C. elegans* that a distinction between altered neuronal migration and cytoskeletal regulation of neuronal activity may be drawn in terms of LIS-1 function. Given the complexity of phenotypes in lissencephaly, it is easy to envision that the epileptic convulsions are likely among the weakest phenotypic manifestations of the fundamental cytoskeletal problems within these neurons. This report leads to a more complete understanding of the underlying consequences of lissencephaly gene defects and their specific contribution to the variable phenotypes comprising this syndrome.

MATERIALS AND METHODS

Worm strains and maintenance

C. elegans growth and maintenance was performed via standard procedures (92). Worm strains used in this study include N2 Bristol, *unc-32(e189) pnm-1(t1550)/qC1 dpy-19(e1259) glp-1(q339) III*; *him-3(e1147)*, *unc-32(e189) III*, *unc-47(e307) III*, *unc-46(e177) V*, *unc-49 (e407) III*, *unc-25(e156) III*, *unc-43(n498 n1186) IV*, *snb-1(md247) V*, *unc-104(e1265) II*, *unc-4(e120) II*, *lin-15(n765ts) X juIs1* (an integrated *unc-25*::SNB-1::GFP strain), *lin-15(n765ts) oxIs12 X* (an integrated *unc-47*::GFP strain), *kyIs161* (an integrated arrestin::GFP strain) and *uIs31* (an integrated *mec-17*::GFP strain).

Genetic crosses were performed by first crossing wild-type N2 males to hermaphrodites carrying GFP constructs and subsequent crosses of these male offspring to hermaphrodites of the target strain. A Zeiss M^2 Bio-Quad fluorescent dissecting microscope was utilized to select GFP positive animals for analysis.

Sequencing of *pnm-1*

Mutant animals homozygous for *pnm-1* were hand-selected as progeny from *pnm-1/+* hermaphrodites on the basis of the *unc-32* marker phenotype. PCR on *pnm-1/pnm-1* worms was performed by standard procedures (93) with the following modifications: 20–30 homozygous *pnm-1* worms were placed into a single PCR tube. PCR was subsequently performed using conditions appropriate for Platinum® Pfx DNA Polymerase (Invitrogen). PCR products, which were short exon segments from genomic DNA, were then subcloned into the pCR®-Blunt vector (Invitrogen) and sequenced using flanking M13 sites within the vector. Sequencing was performed using BigDye® Terminator v3.1 Cycle Sequencing Kit (Applied Biosystems) and ABI PRISM®3100 Genetic Analyzer. The following primer pairs were used in this amplification. pair 1: 5′-CGTCATCGTTTCGTTC GATTCGCGCACTCCG and 3′-TTTTCGTCCGCTTGTCTC AGTAGTAGCTGC; pair 2: 5′-CGTCGATGATGACTCTG TTCGCCTGCTTTTAAG and 3′-AGTGCCTATCGACTT AAAATGCACCCGAAAGCG; pair 3: 5′-CGCTTTCGGGT GCATTTTAAGTCGATAGGCACT and 3′-GAGATCTGGC ACGGTGCCAGCGCATTGAATG; pair 4: 5′-CATTCAAT GCGCTGGCACCGTGCCAGATCTC and 3′-AATGTCGT GTTTTAGTTGGTATAATGG; pair 5: 5′-CCATTATACC AACTAAAACACGACATT and 3′-GATTTCTGATCAA TTTCGACCATAACCACC.

The resulting sequence information was compared to the open-reading frame for *C. elegans lis-1* (T03F6.5) for which we have previously isolated and characterized a cDNA (18).

Rescue of *pnm-1*

The *lis1* cDNA (T03F6.5) was cloned into the vector pJH4.66 at the *Bam* HI sites (removing the GFP::β-tubulin sequence), creating pUA1.1. pUA1.1 and pRF4 [carrying the dominant marker *rol-6(su1006)*] were injected into *pnm-1* heterozygous L4 animals at a concentration of 150 ng/μl. Worms from a stably transmitting line were dissected in 50 μl embryo rinse buffer (40 mM NaCl, 60 mM KCl, 3 mM $MgCl_2$, 3 mM $CaCl_2$ and 10 mM HEPES, pH 7.0) and embryo fixation was performed by standard methods (94). Monoclonal anti-α-tubulin antibody (Sigma) was used at 1:200 and visualized using goat-anti-mouse AlexaFluor488 (Molecular Probes) at 1:800 dilution. DNA was visualized by staining with DAPI. Embryos younger than the 50-cell stage were scored as either having evenly spaced DNA (wild-type) and appropriate spindle structure or clumped DNA and aberrant spindles (mutant).

pnm-1 characterization

The viability, proliferation, size and developmental timing of *pnm-1/pnm-1* worms was characterized. Homozygous *pnm-1* mutant animals were selected at the L2 stage, the earliest stage in which the *unc-32* phenotypic marker is clearly distinguishable, thereby ensuring the selection of homozygous individuals from heterozygous parents for this study. Mutant *unc-32* animals, which are maintained in the homozygous state, were also individually selected at this stage for comparison. In total, 20 L2 homozygotes were isolated to fresh plates and allowed to grow to adulthood at room temperature, which took ∼26 h. This allowed for comparisons of worm growth rate and viability between these two strains, which were almost identical. Additionally, no lethality occurred for either strain during the assay. Morphometeric analysis of these strains was performed to test for size differences in adult homozygous animals to determine whether noticeable proliferation defects were present. Live worms were paralyzed in 3 mM levamisole and placed onto a microscope slide containing a 2% agarose pad and then visually inspected for normal organ structure and photographed for morphometric analysis of body length using MetaMorph software (Universal Imaging Corp.). Size differences were not noted; the mean length of *unc-32* young adult animals was 807.3 μm ($n = 10$) when compared with 797.8 μm for *pnm-1* ($n = 10$) animals.

Immunofluorescence microscopy

To count neuronal nuclei of the ventral nerve cord, young adult animals were fixed in Carnoy's fixative (60% ethanol, 30% acetic acid, 10% chloroform), and following a graduated ethanol rehydration were stained with DAPI. To observe possible alterations in GABA neuronal architecture, *unc-32(e189)* or *pnm-1(t1550)* hermaphrodites were crossed with *lin-15(n765ts) oxIs12 X* males to generate *lin-15(n765ts) oxIs12 X; unc-32(e189)* or *lin-15(n765ts) oxIs12 X;pnm-1(t1550)* animals, respectively. Following minor modification of the methodology of Knobel *et al.* (95), animals were examined for proper extension of axonal processes and branching of commissures; additionally, the number of cell bodies within the ventral nerve cord was scored. To be considered wild-type, the number of commissures scored in each animal was 14–16. Likewise, the number of GABAergic cell bodies considered wild-type within the ventral cord was 20. To examine the final position of the HSN neurons, *unc-32(e189)* or *pnm-1(t1550)* hermaphrodites were crossed with *kyIs161* males to generate *kyIs161;unc-32(e189)* or *kyIs161;pnm-1(t1550)* animals, respectively. Adult animals were examined for the

final position of the HSN neurons. In order to examine migration of the Q-neuroblast lineage, male *uIs31* animals were crossed with either *unc-32(e189)* or *pnm-1(t1550)* animals to generate *uIs31;unc-32(e189)* or *uIs31;pnm-1(t1550)* animals, respectively. Adult animals were examined for wild-type expression of the GFP construct within the AVM and PVM neuronal cell processes (touch cells arising from the Q-neuroblast). To observe GABA vesicle distribution defects, *unc-32(e189)* or *pnm-1(t1550)* hermaphrodites were crossed with *lin-15(n765ts) X juIs1* males to generate *lin-15(n765ts) X juIs1*;*unc-32(e189)* or *lin-15(n765ts) X juIs1;pnm-1(t1550)* animals, respectively. All animals were mounted in 3 mM levamisole on 2% agarose pads for observation with a Nikon Eclipse E800 epifluorescence microscope equipped with DIC optics and Endow GFP HYQ and UV-2E/C DAPI filter cubes (Chroma, Inc.). Analysis was performed at 600–1000× magnification.

Behavioral assays

Convulsion assays were performed by adding 1–10 mg/ml (PTZ) (Sigma) to NGM plates. Drug plates were then seeded with a concentrated stock of OP50 bacteria. Worms were placed onto the drug plates and observed for a period of 30 min. Worms were scored positive for convulsions if they demonstrated repetitive body contractions ('tonic–clonic' convulsions). Animals in this broader class of contractions were subdivided into head-bobbing only, characterized by anterior contractions with posterior immobilization, or as full body contractions, wherein simultaneous contraction of both the anterior and posterior occurred. If animals appeared overtly rigid but still viable (by virtue of pharyngeal activity), and did not respond to touch stimulus following gentle prodding with either a platinum wire or eyebrow hair, they were deemed 'tonic'. As discussed, this latter class of animals was exclusively observed in some of the *dhc-1* (RNAi) experiments. In total, 50 worms of each strain were observed at each concentration of PTZ, unless noted otherwise.

Muscimol paralysis assays were performed as previously described (45) with the following modifications: worms were observed for pharyngeal pumping immediately following placement upon NGM plates seeded with concentrated OP50 containing muscimol (Sigma) at a concentration of 3 mM. If the pharynx continued to pump for 1 h, worms were scored as unresponsive to muscimol; worms responding within the first hour (i.e. no pharyngeal pumping) were scored as responsive to muscimol. A total of 20 worms for each strain were observed.

Digital videos of convulsions

Worms were exposed to 10 mg/ml PTZ for 15 min and then examined under a Zeiss M^2 Bio-Quad stereomicroscope. Convulsions were recorded for 20 s using a Q Imaging Retiga Exi digital video camera at 25 frames/s. The captured images were saved onto an Intel Pentium RAID computer using Northern Eclipse software (Empix Imaging, Mississauga, Ontario). Streaming videos were subsequently converted to QuickTime format at 25 frames/s.

RNA interference

RNA interference by bacterial feeding was performed using standard procedures with minor modifications (60). HT115 (DE3) cells transformed with the L4440 vector containing *dhc-1* sequence (T21E12.4) were inoculated overnight in LB + 100 mg/ml ampicillin. Overnight cultures were plated onto NGM plates containing 100 mg/ml ampicillin and 0.25 mM IPTG. The following day, dauer larvae were placed onto the plates. Young adult offspring of these animals were analyzed for convulsions (N2 animals) muscimol response (N2 animals) or GFP expression using the following marked strains: *lin-15(n765ts) oxIs12 X* (*unc-47::*GFP) or *lin-15(n765ts) X juIs1*(*unc-25::*SNB::GFP).

SUPPLEMENTARY MATERIAL

Supplementary Material is available at HMG Online.

ACKNOWLEDGEMENTS

Special thanks go to Elizabeth Newton and James Thomas for sharing of unpublished data, and whose innovative work served as the impetus for these studies. We also thank all members of the Caldwell Laboratory for their collegiality and teamwork. Particular thanks go to William Dobyns and Erik Jorgensen for their most insightful contributions, as well as Jenny Whitworth for technical assistance. We also thank Lucinda Carnell, Miriam Goodman, Scott Clark, Yun Zhang, Sandhya Koushika, and Cori Bargmann for helpful discussions and suggestions. We are most grateful to David Miller, Steve Von Stetina and Joseph Watson of Vanderbilt University for assistance with ventral cord neuron identification. We appreciatively acknowledge the generosity of Cori Bargmann, Marty Chalfie, Yishi Jin, and Erik Jorgensen for sharing GFP marker strains used in this study, as well as Geraldine Seydoux for the embryonic expression vector, pJH4.66. *C. elegans* strains came from the *Caenorhabditis* Genetics Center, which is funded by the NIH NCRR. Sequencing was performed using equipment funded by the NSF (DBI-0070351). Undergraduate researchers involved in this study (C.J.L. and A.L.B.) were supported by an Undergraduate Science Education Program Grant from the Howard Hughes Medical Institute to The University of Alabama and a grant from The University of Alabama RAC committee. Additional support came from an NSF CAREER Award and a Basil O'Connor Scholar Award from The March of Dimes Birth Defects Foundation to G.A.C.

REFERENCES

1. Dobyns, W.B., Reiner, O., Carrozzo, R. and Ledbetter, D.H. (1993) Lissencephaly. A human brain malformation associated with deletion of the LIS1 gene located at chromosome 17p13. *JAMA*, **23**, 2838–2842.
2. Dobyns, W.B., Stratton, R.F. and Greenberg, F. (1984) Syndromes with lissencephaly. I: Miller–Dieker and Norman–Roberts syndromes and isolated lissencephaly. *Am. J. Med. Genet.*, **18**, 509–526.
3. Reiner, O., Carrozzo, R., Shen, Y., Wehnert, M., Faustinella, F., Dobyns, W.B., Caskey, C.T. and Ledbetter, D.H. (1993) Isolation of a Miller–Dieker lissencephaly gene containing G protein beta-subunit-like repeats. *Nature*, **364**, 717–721.

4. Lo Nigro, C., Chong, C.S., Smith, A.C., Dobyns, W.B., Carrozzo, R. and Ledbetter, D.H. (1997) Point mutations and an intragenic deletion in LIS1, the lissencephaly causative gene in isolated lissencephaly sequence and Miller–Dieker syndrome. *Hum. Mol. Genet.*, **6**, 157–164.
5. Pilz, D.T., Macha, M.E., Precht, K.S., Smith, A.C., Dobyns, W.B. and Ledbetter, D.H. (1998) Fluorescence *in situ* hybridization analysis with LIS1 specific probes reveals a high deletion mutation rate in isolated lissencephaly sequence. *Genet. Med.*, **1**, 29–33.
6. Chong, S.S., Pack, S.D., Roschke, A.V., Tanigami, A., Carrozzo, R., Smith, A.C., Dobyns, W.B. and Ledbetter, D.H. (1997) A revision of the lissencephaly and Miller–Dieker syndrome critical regions in chromosome 17p13.3. *Hum. Mol. Genet.*, **6**, 147–155.
7. Cardoso, C., Leventer, R.J., Ward, H.L., Toyo-Oka, K., Chung, J., Gross, A., Martin, C.L., Allanson, J., Pilz, D.T., Olney, A.H. *et al.* (2003) Refinement of a 400-kb critical region allows genotypic differentiation between isolated lissencephaly, Miller–Dieker syndrome, and other phenotypes secondary to deletions of 17p13.3. *Am. J. Hum. Genet.*, **72**, 918–930.
8. Toyo-oka, K., Shionoya, A., Gambello, M.J., Cardoso, C., Leventer, R., Ward, H.L., Ayala, R., Tsai, L.H., Dobyns, W., Ledbetter, D. *et al.* (2003) 14-3-3epsilon is important for neuronal migration by binding to NUDEL: a molecular explanation for Miller–Dieker syndrome. *Nat. Genet.*, **34**, 274–285.
9. Hattori, M., Adachi, H., Tsujimoto, M., Arai, H. and Inoue, K. (1994) Miller–Dieker lissencephaly gene encodes a subunit of brain platelet-activating factor acetylhydrolase. *Nature*, **370**, 216–218.
10. Ho, Y.S., Swenson, L., Derewenda, U., Serre, L., Wei, Y., Dauter, Z., Hattori, M., Adachi, T., Aoki, J., Arai, H. *et al.* (1997) Brain acetylhydrolase that inactivates platelet-activating factor is a G-protein-like trimer. *Nature*, **385**, 89–93.
11. Hattori, K., Adachi, H., Matsuzawa, A., Yamamoto, K., Tsujimoto, M., Aoki, J., Hattori, M., Arai, H. and Inoue, K. (1996) cDNA cloning and expression of intracellular platelet-activating factor (PAF) acetylhydrolase II. Its homology with plasma PAF acetylhydrolase. *J. Biol. Chem.*, **271**, 33032–33038.
12. Adachi, T., Aoki, J., Manya, H., Asou, H., Arai, H. and Inoue, K. (1997) PAF analogues capable of inhibiting PAF acetylhydrolase activity suppress migration of isolated rat cerebellar granule cells. *Neurosci. Lett.*, **235**, 133–136.
13. Bix, G.J. and Clark, G.D. (1998) Platelet-activating factor receptor stimulation disrupts neuronal migration *in vitro*. *J. Neurosci.*, **18**, 307–318.
14. Xiang, X., Osmani, A.H., Osmani, S.A., Xin, M. and Morris, N.R. (1995) NudF, a nuclear migration gene in *Aspergillus nidulans*, is similar to the human LIS1 gene required for neuronal migration. *Mol. Biol. Cell*, **3**, 297–310.
15. Morris, R. (2000) A rough guide to a smooth brain. *Nat. Cell Biol.*, **2**, E201–E202.
16. Reiner, O. (2000) LIS1. Let's interact sometimes... (part 1). *Neuron*, **28**, 633–636.
17. Liu, Z., Xie, T. and Steward, R. (1999) Lis1, the *Drosophila* homolog of a human lissencephaly disease gene, is required for germline cell division and oocyte differentiation. *Development*, **126**, 4477–4488.
18. Dawe, A.L., Caldwell, K.A., Harris, P.M., Morris, N.R. and Caldwell, G.A. (2001) Evolutionarily conserved nuclear migration genes required for early embryonic development in *Caenorhabditis elegans*. *Dev. Genes Evol.*, **211**, 434–441.
19. Smith, D.S., Niethammer, M., Ayala, R., Zhou, Y., Gambello, M.J., Wynshaw-Boris, A. and Tsai, L.H. (2000) Regulation of cytoplasmic dynein behaviour and microtubule organization by mammalian *Lis1*. *Nat. Cell Biol.*, **2**, 767–775.
20. Faulkner, N.E., Dujardin, D.L., Tai, C.Y., Vaughan, K.T., O'Connell, C.B., Wang, Y. and Vallee, R.B. (2000) A role for the lissencephaly gene LIS1 in mitosis and cytoplasmic dynein function. *Nat. Cell Biol.*, **2**, 784–791.
21. Efimov, V.P. and Morris, N.R. (2000) The LIS1-related NUDF protein of *Aspergillus nidulans* interacts with the coiled-coil domain of the NUDE/RO11 protein. *J. Cell Biol.*, **150**, 681–688.
22. Feng, Y., Olson, E.C., Stukenberg, P.T., Flanagan, L.A., Kirschner, M.W. and Walsh, C.A. (2000) LIS1 regulates CNS lamination by interacting with mNudE, a central component of the centrosome. *Neuron*, **28**, 665–679.
23. Kitagawa, M., Umezu, M., Aoki, J., Koizumi, H., Arai, H. and Inoue, K. (2000) Direct association of LIS1, the lissencephaly gene product, with a mammalian homologue of a fungal nuclear distribution protein, rNUDE. *FEBS Lett.*, **479**, 57–62.
24. Niethammer, M., Smith, D.S., Ayala, R., Peng, J., Ko, J., Lee, M.S., Morabito, M. and Tsai, L.H. (2000) NUDEL is a novel Cdk5 substrate that associates with LIS1 and cytoplasmic dynein. *Neuron*, **28**, 697–711.
25. Sasaki, S., Shionoya, A., Ishida, M., Gambello, MJ., Yingling, J., Wynshaw-Boris, A. and Hirotsune, S. (2000) A LIS1/NUDEL/cytoplasmic dynein heavy chain complex in the developing and adult nervous system. *Neuron*, **28**, 681–696.
26. Swan, A., Nguyen, T. and Suter, B. (1999) *Drosophila* Lissencephaly-1 functions with Bic-D and dynein in oocyte determination and nuclear positioning. *Nat. Cell Biol.*, **7**, 444–449.
27. Aumais, J.P., Tunstead, J.R., McNeil, R.S., Schaar, B.T., McConnell, S.K., Lin, S.H., Clark, G.D. and Yu-Lee, L.Y. (2001) NudC associates with Lis1 and the dynein motor at the leading pole of neurons. *J. Neurosci.*, **21**, RC187, 1–7.
28. Morris, S.M., Albrecht, U., Reiner, O., Eichele, G. and Yu-Lee, L.Y. (1998) The lissencephaly gene product Lis1, a protein involved in neuronal migration, interacts with a nuclear movement protein, NudC. *Curr. Biol.*, **8**, 603–606.
29. Aumais, J.P., Williams, S.N., Luo, W., Nishino, M., Caldwell, K.A., Caldwell, G.A., Lin, S.H. and Yu-Lee, L.Y. (2003) Role for NudC, a dynein-associated nuclear movement protein, in mitosis and cytokinesis. *J. Cell Sci.*, **116**, 1991–2003.
30. Coquelle, F.M., Caspi, M., Cordelieres, F.P., Dompierre, J.P., Dujardin, D.L., Koifman, C., Martin, P., Hoogenraad, C.C., Akhmanova, A., Galjart, N. *et al.* (2002) LIS1, CLIP-170′s key to the dynein/dynactin pathway. *Mol. Cell. Biol.*, **22**, 3089–3102.
31. Sapir, T., Elbaum, M. and Reiner, O. (1997) Reduction of microtubule catastrophe events by LIS1, platelet-activating factor acetylhydrolase subunit. *EMBO J.*, **16**, 6977–6984.
32. Han, G., Liu, B., Zhang, J., Zuo, W., Morris, N.R. and Xiang, X. (2001) The *Aspergillus* cytoplasmic dynein heavy chain and NUDF localize to microtubule ends and affect microtubule dynamics. *Curr. Biol.*, **11**, 719–724.
33. Hirotsune, S., Fleck, M.W., Gambello, M.J., Bix, G.J., Chen, A., Clark, G.D., Ledbetter, D.H., McBain, C.J. and Wynshaw-Boris, A. (1998) Graded reduction of Pafah1b1 (Lis1) activity results in neuronal migration defects and early embryonic lethality. *Nat. Genet.*, **4**, 333–339.
34. Cahana, A., Escamez, T., Nowakowski, R.S., Hayes, N.L., Giacobini, M., von Holst, A., Schumeli, O., Sapir, T., McConnell, S.K., Wurst, W. *et al.* (2001). Targeted mutagenesis of Lis1 disrupts cortical development and LIS1 homodimerization. *Proc. Natl Acad. Sci. USA*, **98**, 6429–6434.
35. Dobyns, W.B., Elias, E.R., Newlin, A.C., Pagon, R.A. and Ledbetter, D.H. (1992) Causal heterogeneity in isolated lissencephaly. *Neurology*, **42**, 1375–1388.
36. White, J., Southgate, E., Thomson, J. and Brenner, S. (1986) The structure of the nervous system of the nematode *Caenorhabditis elegans*. *Phil. Trans. R Soc. Lond.*, **314**, 1–340.
37. Bargmann, C.I. (1998) Neurobiology of the *Caenorhabditis elegans* genome. *Science*, **282**, 2028–2033.
38. Gonczy, P., Schnabel, H., Kaletta, T., Amores, A.D., Hyman, T. and Schnabel, R. (1999) Dissection of cell division processes in the one cell stage *Caenorhabditis elegans* embryo by mutational analysis. *J. Cell Biol.*, **144**, 927–946.
39. Strome, S., Powers, J., Dunn, M., Reese, K., Malone, C.J., White, J., Seydoux, G. and Saxton, W. (2001) Spindle dynamics and the role of gamma-tubulin in early *Caenorhabditis elegans* embryos. *Mol. Biol. Cell*, **12**, 1751–1764.
40. Cardoso, C., Leventer, R.J., Dowling, J.J., Ward, H.L., Chung, J., Petras, K.S., Roseberry, J.A., Weiss, A.M., Das, S., Martin, C.L. *et al.* (2002) Clinical and molecular basis of classical lissencephaly: mutations in the LIS1 gene (PAFAH1B1). *Hum. Mutat.*, **19**, 4–15.
41. Caspi, M., Coquelle, F.M., Koifman, C., Levy, T., Arai, H., Aoki, J., De Mey, J.R. and Reiner, O. (2003) LIS1 missense mutations: variable phenotypes result from unpredictable alterations in biochemical and cellular properties. *J. Biol. Chem.*, **278**, 38740–38748.
42. Cardoso, C., Leventer, R.J., Matsumoto, N., Kuc, J.A., Ramocki, M.B., Mewborn, S.K., Dudlicek, L.L., May, L.F., Mills, P.L., Das, S. *et al.* (2000) The location and type of mutation predict malformation severity in

isolated lissencephaly caused by abnormalities within the LIS1 gene. *Hum. Mol. Genet.*, **9**, 3019–3028.
43. Rocha, L., Briones, M., Ackermann, R.F., Anton, B., Maidment, N.T., Evans, C.J. and Engel, J. Jr. (1996) Pentylenetetrazol-induced kindling: early involvement of excitatory and inhibitory systems. *Epilepsy Res.*, **26**, 105–113.
44. Pujol, N., Bonnerot, C., Ewbank, J.J., Kohara, Y. and Thierry-Mieg, D. (2001) The *Caenorhabditis elegans unc-32* gene encodes alternative forms of a vacuolar ATPase a subunit. *J. Biol. Chem.*, **276**, 11913–11921.
45. McIntire, S.L., Jorgensen, E. and Horvitz, H.R. (1993) Genes required for GABA function in *Caenorhabditis elegans*. *Nature*, **364**, 334–337.
46. McIntire, S.L., Reimer, R.J., Schuske, K., Edwards, R.H. and Jorgensen, E.M. (1997) Identification and characterization of the vesicular GABA transporter. *Nature*, **389**, 870–876.
47. Bamber, B.A., Beg, A.A., Twyman, R.E. and Jorgensen, E.M. (1999) The *Caenorhabditis elegans unc-49* locus encodes multiple subunits of a heteromultimeric GABA receptor. *J. Neurosci.*, **19**, 5348–5359.
48. Miller, D.M., Shen, M.M., Shamu, C.E., Burglin, T.R., Ruvkun, G., Dubois, M.L., Ghee, M. and Wilson, L. (1992) *C. elegans unc-4* gene encodes a homeodomain protein that determines the pattern of synaptic input to specific motor neurons. *Nature*, **355**, 841–845.
49. White, J.G., Southgate, E. and Thomson, J.N. (1992) Mutations in the *Caenorhabditis elegans unc-4* gene alter the synaptic input to ventral cord motor neurons. *Nature*, **355**, 838–841.
50. Reiner, D.J., Newton, E.M., Tian, H. and Thomas, J.H. (1999) Diverse behavioural defects caused by mutations in *Caenorhabditis elegans unc-43* CaM kinase II. *Nature*, **402**, 199–203.
51. Liu, Z., Steward, R. and Luo, L. (2000) *Drosophila* Lis1 is required for neuroblast proliferation, dendritic elaboration and axonal transport. *Nat. Cell Biol.*, **2**, 776–783.
52. Sarnat, H.B. and Flores-Sarnat, L. (2002) Role of Cajal-Retzius and subplate neurons in cerebral cortical development. *Semin. Pediatr. Neurol.*, **9**, 302–308.
53. Zhang, Y., Ma, C., Delohery, T., Nasipak, B., Foat, B.C., Bounoutas, A., Bussemaker, H.J., Kim, S.K. and Chalfie, M. (2002) Identification of genes expressed in *C. elegans* touch receptor neurons. *Nature*, **418**, 331–335.
54. Nonet, M.L. (1999) Visualization of synaptic specializations in live *C. elegans* with synaptic vesicle protein-GFP fusions. *J. Neurosci. Methods*, **89**, 33–40.
55. Jorgensen, E.M., Hartwieg, E., Schuske, K., Nonet, M.L., Jin, Y. and Horvitz, H.R. (1995) Defective recycling of synaptic vesicles in synaptotagmin mutants of *Caenorhabditis elegans*. *Nature*, **378**, 196–199.
56. Zhen, M. and Jin, Y. (1999) The liprin protein SYD-2 regulates the differentiation of presynaptic termini in *C. elegans*. *Nature*, **401**, 371–375.
57. Hoffman, B., Zuo, W., Liu, A. and Morris, N.R. (2001) The LIS1-related protein NUDF of *Aspergillus nidulans* and its interaction partner NUDE bind directly to specific subunits of dynein and dynactin and to α- and γ-tubulin. *J. Biol. Chem.* **276**, 38877–38884.
58. Tai, C.Y., Dujardin, D.L., Faulkner, N.E. and Vallee, R.B. (2002) Role of dynein, dynactin and CLIP-170 interactions in LIS1 kinetochore function. *J. Cell Biol.*, **156**, 959–968.
59. Gonczy, P., Pichler, S., Kirkham, M. and Hyman, A.A. (1999b) Cytoplasmic dynein is required for distinct aspects of MTOC positioning, including centrosome separation, in the one cell stage *Caenorhabditis elegans* embryo. *J. Cell Biol.*, **147**, 135–150.
60. Timmons, L., Court, D.L. and Fire, A. (2001) Ingestion of bacterially expressed dsRNAs can produce specific and potent genetic interference in *Caenorhabditis elegans*. *Gene*, **263**, 103–112.
61. Koushika, S.P., Schaefer, A.M., Vincent, R., Willis, J.H., Bowerman, B. and Nonet, M.L. (2004) Mutations in *Caenorhabditis elegans* cytoplasmic dynein components reveal specificity of neuronal retrograde cargo. *J. Neurosci.*, **24**, 3907–3916.
62. Okada, Y., Yamazaki, H., Sekine-Aizawa, Y. and Hirokawa. N. (1995) The neuron-specific kinesin superfamily protein KIF1A is a unique monomeric motor for anterograde axonal transport of synaptic vesicle precursors. *Cell*, **81**, 769–780.
63. Hall, D.H. and Hedgecock, E.M. (1991) Kinesin-related gene *unc-104* is required for axonal transport of synaptic vesicles in *C. elegans*. *Cell*, **65**, 837–847.
64. Nonet M.L., Saifee O., Zhao H., Rand J.B. and Wei L. (1998) Synaptic transmission deficits in *Caenorhabditis elegans* synaptobrevin mutants. *J. Neurosci.*, **18**, 70–80.
65. Crino, P.B., Miyata, H. and Vinters, H.V. (2002) Neurodevelopmental disorders as a cause of seizures: neuropathologic, genetic and mechanistic considerations. *Brain Pathol.*, **12**, 212–233.
66. Shmueli, O., Cahana, A. and Reiner, O. (1999) Platelet-activating factor (PAF) acetylhydrolase activity, LIS1 expression and seizures. *J. Neurosci. Res.*, **57**, 176–184.
67. Ross, M.E. (2002) Brain malformations, epilepsy and infantile spasms. *Int. Rev. Neurobiol.*, **49**, 333–352.
68. Chalfie, M., Dean, E., Reilly, E. Buck, K. and Thomson, J.N. (1986) Mutations affecting microtubule structure in *Caenorhabditis elegans*. *J. Cell Sci. Suppl.*, **5**, 257–271.
69. Hafezparast, M., Klocke, R., Ruhrberg, C., Marquardt, A., Ahmad-Annuar, A., Bowen, S., Lalli, G., Witherden, A.S., Hummerich, H., Nicholson, S. *et al.* (2003) Mutations in dynein link motor neuron degeneration to defects in retrograde transport. *Science*, **300**, 808–812.
70. Puls, I., Jonnakuty, C., LaMonte, B.H., Holzbaur, E.L., Tokito, M., Mann, E., Floeter, M.K., Bidus, K., Drayna, D., Oh, S.J. *et al.* (2003) Mutant dynactin in motor neuron disease. *Nat. Genet.*, **33**, 455–456.
71. Schuyler, S.C. and Pellman, D. (2001) Microtubule 'plus-end tracking proteins': The end is just the beginning. *Cell*, **105**, 421–424.
72. Vaughan, K.T., Tynan, S.H., Faulkner, N.E., Echeverri, C.J. and Valle, R.B. (1999) Colocalization of cytoplasmic dynein with dynactin and CLIP-170 at microtubule distal ends. *J. Cell Sci.*, **112**, 1437–1447.
73. Vaughan, P.S., Miura, P., Henderson, M., Byrne, B. and Vaughan, K.T. (2002) A role for regulated binding of p150(Glued) to microtubule plus ends in organelle transport. *J. Cell Biol.*, **158**, 305–319.
74. Valetti, C., Wetzel, D.M., Schrader, M., Hasbani, M.J., Gill, S.R., Kreis, T.E. and Schroer, T.A. (1999) Role of dynactin in endocytic traffic: effects of dynamitin overexpression and colocalization with CLIP-170. *Mol. Biol. Cell*, **10**, 4107–4120.
75. Habermann, A., Schroer, T.A., Griffiths, G. and Burkhardt, J.K. (2001) Immunolocalization of cytoplasmic dynein and dynactin subunits in cultured macrophages: enrichment on early endocytic organelles. *J. Cell Sci.*, **114**, 229–240.
76. Zhang, J., Li, S., Fisher, R. and Xiang, X. (2003) Accumulatin of cytoplasmic dynein and dynactin at microtubule plus ends in *Apergillus nidulans* is kinesin dependent. *Mol. Biol. Cell*, **14**, 1479–1488.
77. Bowman, A.B., Patel-King, R.S., Benashski, S.E., McCaffery, J.M., Goldstein, L.S. and King, S.M. (1999) *Drosophila* roadblock and *Chlamydomonas* LC7: a conserved family of dynein-associated proteins involved in axonal transport, flagellar motility and mitosis. *J. Cell Biol.*, **146**, 165–180.
78. Martin, M., Iyadurai, S.J., Gassman, A., Gindhart, J.G., Jr, Hays, T.S. and Saxton, W.M. (1999) Cytoplasmic dynein, the dynactin complex and kinesin are interdependent and essential for fast axonal transport. *Mol. Biol. Cell*, **10**, 3717–3728.
79. Duncan, J.E. and Warrior, R. (2002) The cytoplasmic dynein and kinesin motors have interdependent roles in patterning the *Drosophila* oocyte. *Curr. Biol.*, **12**, 1982–1991.
80. Brady, S.T., Pfister, K.K. and Bloom, G.S. (1990) A monoclonal antibody against kinesin inhibits both anterograde and retrograde fast axonal transport in squid axoplasm. *Proc. Natl Acad. Sci. USA*, **87**, 1061–1065.
81. Waterman-Storer, C.M., Karki, S.B., Kuznetsov, S.A., Tabb, J.S., Weiss, D.G., Langford, G.M. and Holzbaur, E.L. (1997) The interaction between cytoplasmic dynein and dynactin is required for fast axonal transport. *Proc. Natl Acad. Sci. USA*, **94**, 12180–12185.
82. Garcia, C.C., Blair, H.J., Seager, M., Coulthard, A., Tennant, S., Buddles, M., Curtis, A. and Goodship, J.A. (2004) Identification of a mutation in synapsin I, a synaptic vesicle protein, in a family with epilepsy. *J. Med. Genet.*, **41**, 183–187.
83. Li, L., Chin, L.S., Shupliakov, O., Brodin, L., Sihra, T.S., Hvalby, O., Jensen, V., Zheng, D., McNamara, J.O., Greengard, P. and Andersen, P. (1995) Impairment of synaptic vesicle clustering and of synaptic transmission, and increased seizure propensity, in synapsin I-deficient mice. *Proc. Natl Acad. Sci. USA*, **92**, 9235–9239.
84. Di Paolo, G., Sankaranarayanan, S., Wenk, M.R., Daniell, L., Perucco, E., Caldarone, B.J., Flavell, R., Picciotto, M.R., Ryan, T.A., Cremona, O. and De Camilli, P. (2002) Decreased synaptic vesicle recycling efficiency and cognitive deficits in amphiphysin 1 knockout mice. *Neuron*, **33**, 789–804.

85. Pierre, P., Scheel, J., Rickard, J.E. and Kreis, T.E. (1992) CLIP-170 links endocytic vesicles to microtubules. *Cell*, **70**, 887–900.
86. Burkhardt, J.K., Echeverri, C.J., Nilsson, T. and Vallee, R.B. (1997) Overexpression of the dynamitin (p50) subunit of the dynactin complex disrupts dynein-dependent maintenance of membrane organelle distribution. *J. Cell Biol.*, **139**, 469–484.
87. Dhani, S.U., Mohammad-Panah, R., Ahmed, N., Ackerley, C., Ramjeesingh, M. and Bear, C.E. (2003) Evidence for a functional interaction between the ClC-2 chloride channel and the retrograde motor dynein complex. *J. Biol. Chem.*, **278**, 16262–16270.
88. Haug, K., Warnstedt, M., Alekov, A.K., Sander, T., Ramirez, A., Poser, B., Maljevic, S., Hebeisen, S., Kubisch, C., Rebstock, J. *et al.* (2003) Mutations in CLCN2 encoding a voltage-gated chloride channel are associated with idiopathic generalized epilepsies. *Nat. Genet.*, **33**, 527–532.
89. Clark, G.D., Mizuguchi, M., Antalffy, B., Barnes, J. and Armstrong, D. (1997) Predominant localization of the LIS family of gene products to Cajal-Retzius cells and ventricular neuroepithelium in the developing human cortex. *J. Neuropathol. Exp. Neurol.*, **9**, 1044–1052.
90. Treiman, D.M. (2001) GABAergic mechanisms in epilepsy. *Epilepsia*, **42** (Suppl. 3), 8–12.
91. Chagnac-Amitai, Y. and Connors, B.W. (1989) Horizontal spread of synchronized activity in neocortex and its control by GABA-mediated inhibition. *J. Neurophysiol.* **61**, 747–758.
92. Brenner, S. (1974) The genetics of *Caenorhabditis elegans*. *Genetics*, **77**, 71–94.
93. Barstead, R.J., Kleiman, L. and Waterston, R.H. (1991) Cloning, sequencing, and mapping of an alpha-actinin gene from the nematode *Caenorhabditis elegans*. *Cell Motil. Cytoskeleton*, **20**, 69–78.
94. Guo, S. and Kemphues, K.J. (1995) *par-1*, a gene required for establishing polarity in *C. elegans* embryos, encodes a putative Ser/Thr kinase that is asymmetrically distributed. *Cell*, **81**, 611–620.
95. Knobel, K.M., Davis, W.S., Jorgensen, E.M. and Bastiani, M.J. (2001) UNC-119 suppresses axon branching in *C. elegans*. *Development*, **128**, 4079–4092.
96. Emes, R.D. and Ponting, C.P. (2001) A new sequence motif linking lissencephaly, Treacher Collins and oral-facial-digital type 1 syndromes, microtubule dynamics and cell migration. *Hum. Mol. Genet.*, **10**, 2813–2820.